



*Accepted
1/11/00
8/29/00*

Reconfigurable GPS Antenna

K. W. Lee and R. G. Rojas

The Ohio State University

ElectroScience Laboratory

Department of Electrical Engineering
1320 Kinnear Road
Columbus, Ohio 43212

Final Report 737675-2
Grant No. F49620-99-1-0218
August 2000

U.S. Air Force, AFOSR/NM
801 N. Randolph St., Room 732
Arlington, VA 22203-1977

DTIC QUALITY INSPECTED 4

20001016 056

A. Approved for public release; Distribution is unlimited

REPORT DOCUMENTATION PAGE

Form Approved
GSA FPMR (41 CFR) 101-11.6

Public reporting burden for this collection of information is estimated to average 1 hour per response, including reviewing the data needed, and completing and reviewing the collection of information. Send comments regarding this burden estimate or any other aspect of this collection of information, including suggestions for reducing this burden, to Washington Headquarters Services, Directorate for Information Operations and Reports, 1215 Jefferson Davis Highway, Suite 1204, Arlington, VA 22202-4302, and to the Office of Management and Budget, Paperwork Reduction Project (0704-0188).

AFRL-SR-BL-TR-00-

1. AGENCY USE ONLY (Leave blank)	2. REPORT DATE August 2000	3. REPORT TYPE AND DATES COVERED Final
4. TITLE AND SUBTITLE Reconfigurable GPS Antenna		
6. AUTHOR(S) K.W. Lee and R.G. Rojas		
7. PERFORMING ORGANIZATION NAME(S) AND ADDRESS(ES) The Ohio State University ElectroScience Laboratory 1320 Kinnear Road Columbus, OH 43212		
8. PERFORMING ORGANIZATION REPORT NUMBER 737675-2		
9. SPONSORING/MONITORING AGENCY NAME(S) AND ADDRESS(ES) U.S. Air Force, AFOSR/NM 801 N. Randolph St., Room 732 Arlington, VA 22203-1977		
10. SPONSORING/MONITORING AGENCY REPORT NUMBER F49620-99-1-0218		
11. SUPPLEMENTARY NOTES		
12a. DISTRIBUTION AVAILABILITY STATEMENT Approve for public release; distribution is unlimited.		
12b. DISTRIBUTION CODE		
13. ABSTRACT (Maximum 200 words) Various schemes for the design of reconfigurable printed antenna elements are presented for GPS and other applications. The antenna elements can be linearly or circularly polarized. The physical phenomenon behind these schemes is based on the modification of the EM propagation characteristics of a dielectric substrate by using parasitic metallic strips connected by switches. The switches can be implemented with diodes, transistors or RF MEMS. The switches effectively change the dimensions of the metallic strips causing the radiation of surface waves supported within the substrate. The radiation patterns can be changed in real time by turning the switches on or off. An reconfigurable linearly polarized printed antenna is obtained by using four strips near all four edges of the antenna. On the other hand, a circularly polarized antenna requires a ring completely surrounding the antenna element. To reduce the overall size of the antenna, an alternative configuration having a smaller ground plane and ring is presented. Simulated results, obtained with a FDTD code, are obtained to assess the performance of the various designs.		
14. SUBJECT TERMS		
15. NUMBER OF PAGES 57		
16. PRICE CODE		
17. SECURITY CLASSIFICATION OF REPORT unclassified	18. SECURITY CLASSIFICATION OF THIS PAGE unclassified	19. SECURITY CLASSIFICATION OF ABSTRACT unclassified
20. LIMITATION OF ABSTRACT unlimited		

Contents

List of Figures	iv
1 Introduction	1
1.1 Overview	1
1.2 Technology Transition	6
2 Linearly Polarized Antenna Element	8
2.1 Introduction	8
2.2 Parametric Study - Strip Width	9
2.3 Parametric Study - Strip Length	9
2.4 Parametric Study - Strip Separation	11
2.5 Reconfigurable Antenna Element	12
3 Circularly Polarized Antenna: Large Ground Plane Case	17
3.1 Introduction	17
3.2 Parametric Study - Ring Width	17
3.3 Parametric Study - Ring Separation	19
3.4 Reconfigurable Antenna Element: L2 GPS Frequency	22
3.5 Reconfigurable Antenna at L1 GPS Frequency	23
4 Circularly Polarized Antenna: Small Ground Plane Case	32
4.1 Introduction	32
4.2 Preliminary Analysis	33
4.3 Design of Metallic Ring for Simultaneous Operation at L1/L2 Frequencies	40
5 Summary and Conclusions	47
5.1 Accomplishments	47
5.2 Suggestions for Future Work	48
Bibliography	50

List of Figures

1.1	Linearly polarized microstrip antenna with an array of diode-loaded metal strips along the radiating edges of the patch (top view)	3
1.2	Linearly polarized microstrip antenna with an array of (a) metallic strips and (b) an array of diode-loaded metallic strips around the patch (top view)	4
1.3	Circularly polarized microstrip antenna with (a) a metallic ring and (b) an array of diode-loaded metallic strips (top view)	5
1.4	Circularly polarized microstrip antenna with ground plane that is smaller than the metallic-ring around the patch	6
1.5	Circularly polarized microstrip antenna with small ground plane and diode-loaded metallic rings around the patch (top view)	7
2.1	Parametric Study - Strip Width: four-strip antenna E-plane pattern with $S_1 = 0.3\lambda_d$, $l_1 = 1.0\lambda_d$ and W_1 varies from 0.8 to $1.2\lambda_d$	10
2.2	Parametric Study - Strip Width: four-strip antenna H-plane pattern with $S_1 = 0.3\lambda_d$, $l_1 = 1.0\lambda_d$ and W_1 varies from 0.8 to $1.2\lambda_d$	10
2.3	Parametric Study - Strip Length: four-strip antenna E-plane pattern with $S_1 = 0.4\lambda_d$, $W_1 = 1.0\lambda_d$ and l_1 varies from 0.8 to $1.2\lambda_d$	11
2.4	Parametric Study - Strip Length: four-strip antenna H-plane pattern with $S_1 = 0.4\lambda_d$, $W_1 = 1.0\lambda_d$ and l_1 varies from 0.8 to $1.2\lambda_d$	12
2.5	Parametric Study - Strip Separation: four-strip antenna E-plane pattern with $l_1 = 0.8\lambda_d$, $W_1 = 1.0\lambda_d$ and S_1 varies from 0.2 to $0.4\lambda_d$	13
2.6	Parametric Study - Strip Separation: four-strip antenna H-plane pattern with $l_1 = 0.8\lambda_d$, $W_1 = 1.0\lambda_d$ and S_1 varies from 0.2 to $0.4\lambda_d$	13
2.7	Calculated E-plane radiation pattern for design 1	15
2.8	Calculated H-plane radiation pattern for design 1	15
2.9	Calculated E-plane radiation pattern for design 2	16
2.10	Calculated H-plane radiation pattern for design 2	16
3.1	Parametric Study - Ring Width: - E_{RHCP} antenna pattern in $\phi = \pm 90^\circ$ plane with $S_1 = 0.4 \lambda_d$ and W_1 varies from 0.6 to $1.2 \lambda_d$	18
3.2	Parametric Study - Ring Width: - E_{LHCP} antenna pattern in $\phi = \pm 90^\circ$ plane with $S_1 = 0.4 \lambda_d$ and W_1 varies from 0.6 to $1.2 \lambda_d$	19
3.3	Parametric Study - Ring Width: - E_{RHCP} antenna pattern in $\phi = 0^\circ - 180^\circ$ plane with $S_1 = 0.4 \lambda_d$ and W_1 varies from 0.6 to $1.2 \lambda_d$	20

3.4	Parametric Study - Ring Width: - E_{LHCP} antenna pattern in $\phi = 0^\circ - 180^\circ$ plane with $S_1 = 0.4 \lambda_d$ and W_1 varies from 0.6 to $1.2 \lambda_d$. .	20
3.5	Parametric Study - Ring Separation: - E_{RHCP} antenna pattern in $\phi = \pm 90^\circ$ plane with $W_1 = 1.0 \lambda_d$ and S_1 varies from 0.2 to $0.6 \lambda_d$	21
3.6	Parametric Study - Ring Separation: - E_{LHCP} antenna pattern in $\phi = \pm 90^\circ$ plane with $W_1 = 1.0 \lambda_d$ and S_1 varies from 0.2 to $0.6 \lambda_d$	21
3.7	Calculated E_{RHCP} antenna pattern at $\phi = 90^\circ$ and $f = 1.227$ GHz for the adaptive circularly polarized patch antenna (Design 1).	24
3.8	Calculated E_{LHCP} antenna pattern in $\phi = \pm 90^\circ$ plane at $f = 1.227$ GHz for the adaptive circularly polarized patch antenna (Design 1).	25
3.9	Calculated E_{RHCP} antenna pattern in $\phi = \pm 90^\circ$ plane at $f = 1.575$ GHz for the adaptive circularly polarized patch antenna (Design 1).	26
3.10	Calculated E_{LHCP} antenna pattern in $\phi = \pm 90^\circ$ plane at $f = 1.575$ GHz for the adaptive circularly polarized patch antenna (Design 1).	27
3.11	Calculated E_{RHCP} antenna pattern in $\phi = \pm 90^\circ$ plane at $f = 1.575$ GHz for the adaptive circularly polarized patch antenna (Design 2).	28
3.12	Calculated E_{LHCP} antenna pattern in $\phi = \pm 90^\circ$ plane at $f = 1.575$ GHz for the adaptive circularly polarized patch antenna (Design 2).	29
3.13	Calculated E_{RHCP} antenna pattern in $\phi = \pm 90^\circ$ plane at $f = 1.227$ GHz for the adaptive circularly polarized patch antenna (Design 2).	30
3.14	Calculated E_{LHCP} antenna pattern in $\phi = \pm 90^\circ$ plane at $f = 1.227$ GHz for the adaptive circularly polarized patch antenna (Design 2).	31
4.1	Geometry for (a) dielectric slab waveguide without a ground plane and (b) grounded dielectric waveguide	34
4.2	Preliminary analysis on the effect of the ground plane dimensions (L_3 , L_4) on the radiation pattern, L1 band	35
4.3	Radiation pattern of E_{RHCP} in $\pm 90^\circ$ plane as a function of ring dimensions l_1 and l_2 , L2 band	36
4.4	Radiation pattern of E_{RHCP} in $0^\circ - 180^\circ$ plane as a function of ring dimensions l_1 and l_2 , L2 band	37
4.5	Radiation pattern of E_{RHCP} in $\pm 90^\circ$ plane as a function of ring dimensions l_1 and l_2 , L1 band	38
4.6	Radiation pattern of E_{RHCP} in $0^\circ - 180^\circ$ plane as a function of ring dimensions l_1 and l_2 , L1 band	39
4.7	Calculated E_{RHCP} antenna pattern in $\phi = \pm 90^\circ$ plane at $f = 1.227$ GHz	41
4.8	Calculated E_{RHCP} antenna pattern in $\phi = \pm 90^\circ$ plane at $f = 1.575$ GHz	42
4.9	Calculated E_{LHCP} antenna pattern at $\phi = \pm 90^\circ$ at $f = 1.227$ GHz . .	43
4.10	Calculated E_{LHCP} antenna pattern at $\phi = \pm 90^\circ$ at $f = 1.575$ GHz . .	43
4.11	Calculated E_{RHCP} antenna pattern in $\phi = 0^\circ - 180^\circ$ plane at $f = 1.227$ GHz	44
4.12	Calculated E_{RHCP} antenna pattern in $\phi = 0^\circ - 180^\circ$ plane at $f = 1.575$ GHz	45
4.13	Calculated E_{LHCP} antenna pattern in $\phi = 0^\circ - 180^\circ$ plane at $f = 1.227$ GHz	46

4.14	Calculated E_{LHCP} antenna pattern in $\phi = 0^\circ - 180^\circ$ plane at $f =$ 1.575 GHz	46
------	---	----

Chapter 1

Introduction

1.1 Overview

High performance GPS receiving antennas (able to operate at 1.227 and 1.575 GHz) are in large demand due to the extensive use of the global positioning system (GPS) in navigation and landing systems[1]. Since the GPS satellites transmit right-handed circularly polarized (RHCP) signals, the rejection of the cross polarized (left-handed circularly polarized, LHCP) signal is important to avoid multi-path problems. A GPS antenna must also have a hemispherical coverage to receive signals from as many satellites as possible. Printed antennas (microstrip patches, dipoles, bow ties, etc.) are one class of antennas heavily used for this application. They have several advantages over other antennas, such as lightweight, low cost, low profile, conformity to surface, compatible with printed circuit technology, direct integrability with microwave circuitry, etc. If designed correctly, a microstrip patch antenna can produce a broad beam in the upper hemisphere. This satisfies the required hemispherical coverage for GPS applications. To operate at the L1 and L2 GPS frequencies, it is common to use dual frequency patches [2, 3]. However, one can also use a wideband RHCP antenna that covers both GPS frequencies. Various designs for this type of printed antenna can be found in the literature.

In addition to the above requirements, there are applications where a GPS antenna must be able to modify its pattern in the neighborhood of the horizon to avoid receiving unwanted (jamming) signals. The conventional approach to handle jamming

signals is to use an adaptive array to cancel the unwanted signal. However, the approach proposed here is based on the use of a reconfigurable antenna element that can modify its pattern in real time. The concept of reconfigurable antenna elements is the subject of intense research, partly due to the development of RF MEMS that can be used as switches [4]. The switches are used to modify the shape/size of the antenna element and thus change its radiation pattern. The scheme presented here falls into the category of reconfigurable antennas because we propose to use switches to change the widths of parasitic strips and modify the radiation pattern of a microstrip patch in real time. In this report we refer to the switches as diodes, however, the switches can be implemented with diodes, transistors or MEMS.

Previously, we presented a scheme to adaptively control the surface waves excited within the dielectric substrate to modify the antenna radiation pattern [5]. The concept is based on the idea of using an array of diode-loaded metallic strips mounted on the same substrate as the microstrip antenna as depicted in Figure 1.1. The diodes are being used as electrical switches and are assumed to have two operating stages. Ideally, the “on” stage allows the currents to flow, while the “off” stage does not allow any current flow through the diode. The resultant reconfigurable antenna has the ability to selectively change its radiation pattern depending on the operating stage of the diodes. The configuration shown in Figure 1.1, where metallic strips are placed along the radiating edges of the linearly polarized antenna, has the ability to control its E-plane radiation pattern while minimizing any changes in the H-plane radiation pattern [6].

The ability to control both the E- and H-plane patterns by placing strips around the patch antenna (along the radiating edges and non-radiating edges) is important for practical applications and is discussed in Chapter 2 and the proposed scheme is shown in Figure 1.2. It has been found that the width and length of the strips are the most critical parameters of the design. [7] It is also noticed that there is a strong coupling between the patch and the four strips if the spacing (between the patch and each strip) is less than approximately $0.2\lambda_d$. As in the case depicted in Figure 1.1, the radiation pattern of the antenna shown in Figure 1.2 can be changed dramatically by

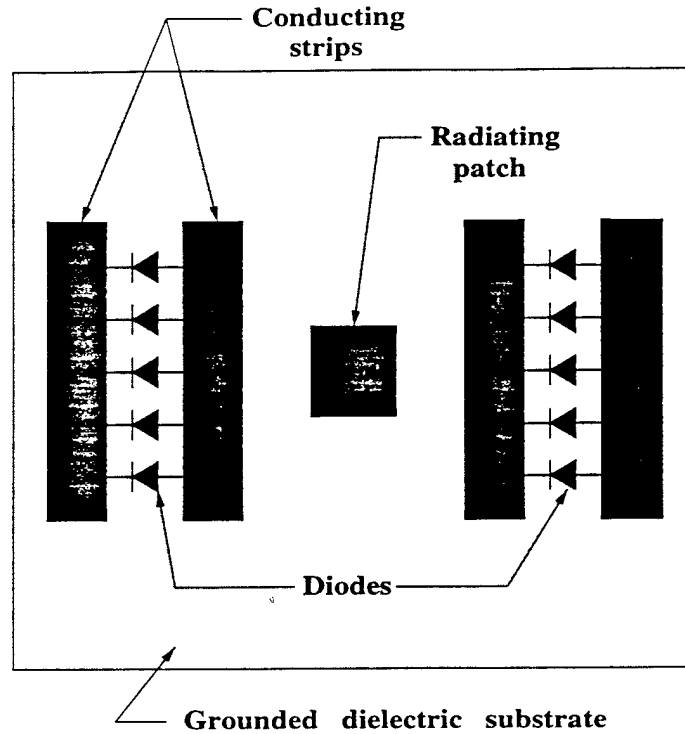


Figure 1.1: Linearly polarized microstrip antenna with an array of diode-loaded metal strips along the radiating edges of the patch (top view)

varying the width of the four strips. However, the length of the strips also becomes important in this latter case. The reason for this behavior can be easily explained by comparing the two configurations (Figure 1.1 and Figure 1.2). The length of the strips in Figure 1.1 can be extended further, and it is found that the strip length has a small effect on the radiation pattern when it is greater than approximately $1.2\lambda_d$. On the other hand, the length of the strips in Figure 1.2 cannot be extended further because the strips will eventually come into electrical contact (touch each other) as their lengths increase. This is undesirable because the current distribution on the four strips can change dramatically when they become electrically connected and will modify the radiation pattern.

As mentioned before, GPS satellites transmit RHCP signals, and hence, the receiving antenna must also be RHCP. Thus, it is necessary to investigate the ability to control the radiation pattern of a circularly polarized antenna with the scheme proposed here. This is done in Chapter 3 and the scheme is shown in Figure 1.3. The

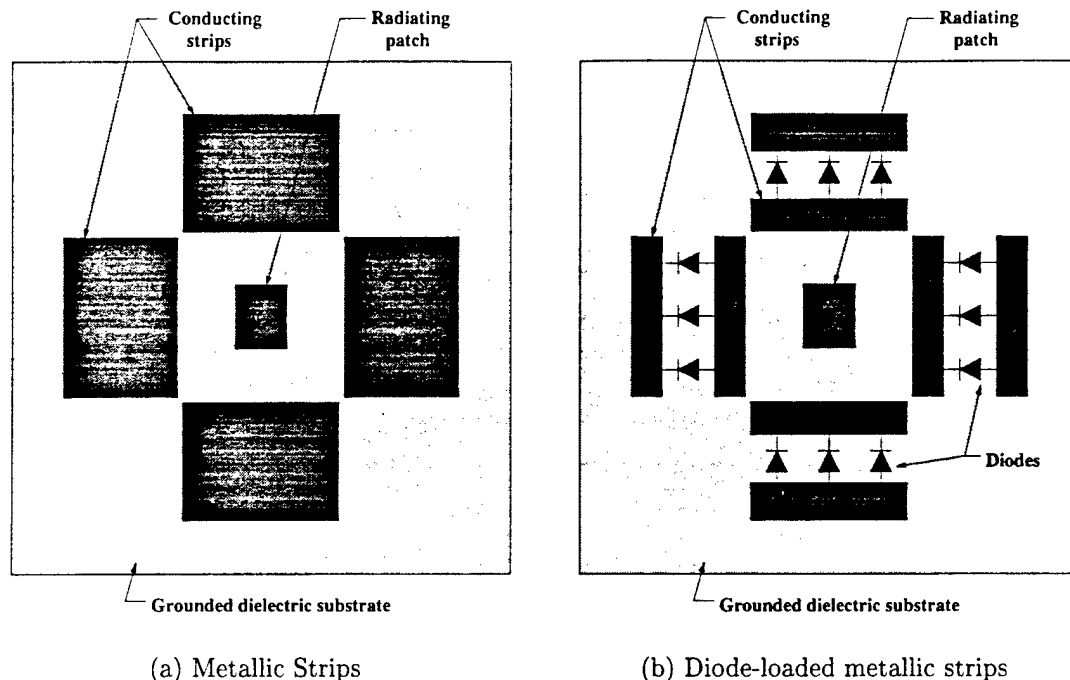


Figure 1.2: Linearly polarized microstrip antenna with an array of (a) metallic strips and (b) an array of diode-loaded metallic strips around the patch (top view)

main difference between the configurations for the linearly and circularly polarized antennas is that in the latter case all the strips are in electrical contact forming a ring around the patch. This is expected because the patch is radiating at all four edges for circular polarization. Hence, a symmetric structure around the patch is required to contribute equally to the radiation pattern.

One disadvantage of the above configurations is the overall size of the antenna element. In order to reduce the size other schemes need to be explored. One such scheme is presented in Chapter 4. The reconfigurable antenna discussed in that chapter, which is depicted in Figure 1.4 and 1.5, has a smaller overall size.

With this new scheme the metallic ring is able to control the antenna pattern beamwidth at both GPS frequencies simultaneously. The idea is based on increasing the strength of the surface waves which in turn decreases the width of the metallic ring and yields a smaller structure. The results presented in Chapter 4 are preliminary because further study is needed to fully understand the behavior of this antenna.

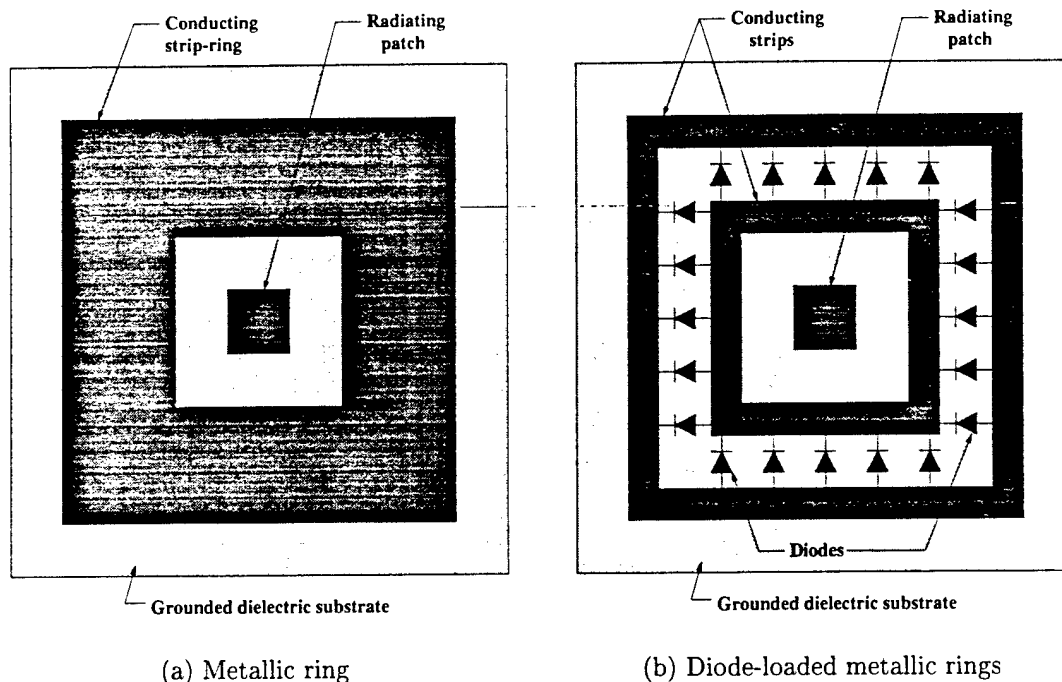


Figure 1.3: Circularly polarized microstrip antenna with (a) a metallic ring and (b) an array of diode-loaded metallic strips (top view)

Finally, in Chapter 5 some concluding remarks are given and the future direction for this research topic is discussed.

Another important consideration that needs to be considered is the applicability of the above reconfigurable antenna elements for array applications. The initial motivation for this research was the development of a reconfigurable antenna element that could replace an adaptive array. If the antenna elements proposed here were to be used in an array, they would be designed with a high gain (narrow beamwidth) to avoid the problem of grating lobes. In other words, a reconfigurable antenna element would play the role of a sub-array in a large array configuration.

Note that all the antenna configurations in this report are analyzed with a 3-D finite difference time domain (FDTD) code developed at the ElectroScience Laboratory [8]. In this study, the “on” stage of the switches is modeled by thin wires connecting the metallic strips. When the switches are “off”, the thin wires are removed from the model. Obviously this model assumes the switches are ideal. A more

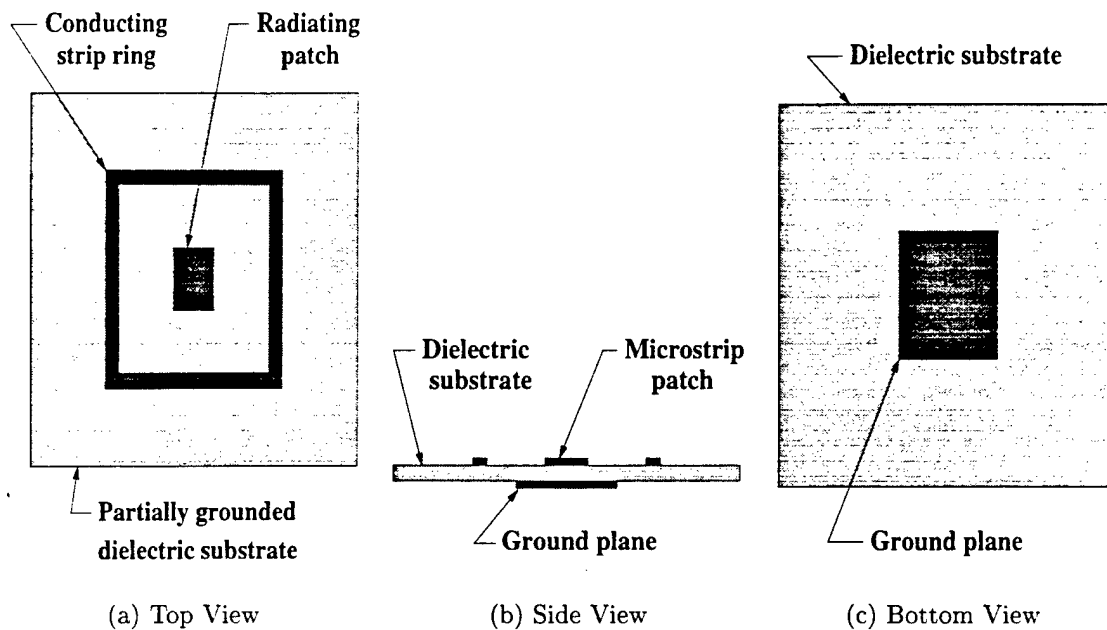


Figure 1.4: Circularly polarized microstrip antenna with ground plane that is smaller than the metallic-ring around the patch

realistic model would have to take into account the actual performance of the switch being used (diode, MEMS, etc.).

1.2 Technology Transition

- Customer: Mr. Todd Jenkins
AFRL/SNAR
Reference Systems Branch
2241 Avionics Circle Suite 19
WPAFB OH 45433-7321

Voice: (937)255-5668 / DSN 785-5668 x4138
Fax: (937)656-4301 / DSN 786-4301
E-mail: Todd.Jenkins@sn.wpafb.af.mil

- Results: Reconfigurable printed antenna element (linearly and circularly polarized) whose radiation pattern can be modified in real time.
- Application: GPS applications in the presence of jamming signals

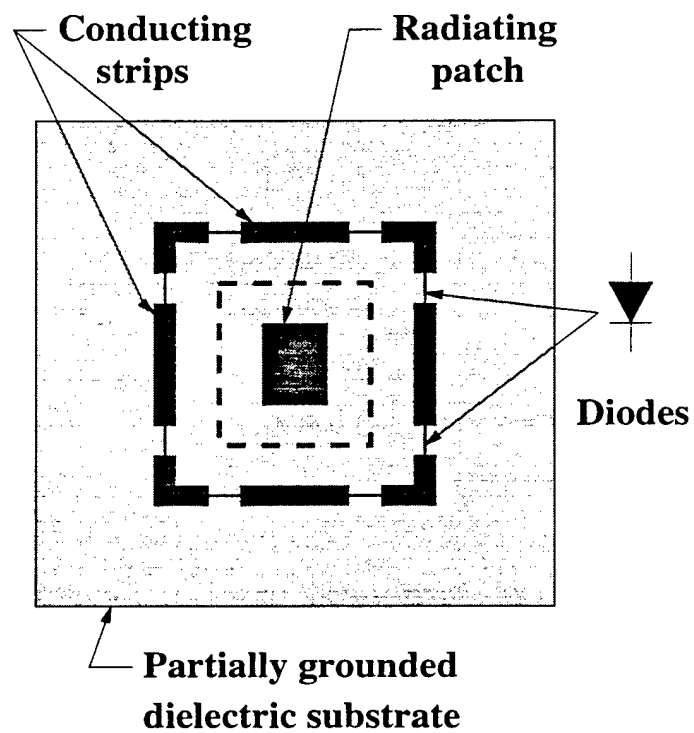


Figure 1.5: Circularly polarized microstrip antenna with small ground plane and diode-loaded metallic rings around the patch (top view)

Chapter 2

Linearly Polarized Antenna Element

2.1 Introduction

The design procedure for typical linearly polarized rectangular microstrip antennas can be found in the literature [2, 3, 9]. The analysis and design of the parasitic strips (width, length, spacing) for strips along the radiating edges of the patch (Fig. 1.1) are carried out in [6]. In that report, we showed the ability of diode-loaded metallic-strips to adaptively control surface waves, and therefore, modify the E-plane radiation pattern.

In this chapter, a scheme that is able to control both the E- and H-plane patterns of a linearly polarized patch antenna using surface waves is presented. The antenna plus the parasitic strips are shown in Figure 1.2, A parametric study is conducted to determine the effect of the various strip parameters (width, length and separation from patch) on the radiation patterns. Finally, two design examples are presented to show the significant changes that can be achieved in the radiation patterns in both the E- and H-planes by effectively changing the strip dimensions using a set of switches. As mentioned before, this type of antenna is referred to as a reconfigurable antenna.

The following parametric study is important in the design of a reconfigurable antenna element. The information gained with this study will be used to design the parasitic strips and the optimal placement of the switches.

2.2 Parametric Study - Strip Width

In this section, the effect of the strip width on the antenna performance is investigated. In a parametric study of the width of a pair of strips (one on each side of the radiating edges of the patch) conducted in [6], it was shown that when the strip width is electrically small, the substrate and parasitic strips act like a surface wave guiding structure, making the surface waves stronger which distort the radiation pattern. However, when the strip width becomes electrically large, this guiding structure no longer supports surface waves, it supports leaky waves. Energy leaks out and contributes constructively to the main-beam. Therefore, the resultant antenna pattern has a higher gain and lower side and back lobes. Note that in the analysis carried in [6], the strip length was assumed to be infinitely long (2-D model). Since we cannot use 2-D models for the four strip case, we are forced to use 3-D models using a 3-D FDTD code.

If we carefully examine Figures 2.1 and 2.2, we observe that the antenna patterns do not change significantly when the strip width is electrically small. When the strip width increases to approximately λ_d (λ_d = wavelength inside substrate), the resultant patterns show dramatical changes. The above phenomena is similar to the two-strip case [6]. However, the antenna patterns in this case start to change again when the width of the strips continue to increase beyond a certain point. This is not the same effect as in the two-strip case where the antenna patterns stay fairly constant as the strip width continues to increase beyond a certain critical dimension. Hence, it can be concluded that the length of all four strips, including the strips along the non-radiating edges have a strong effect on the resultant antenna patterns.

2.3 Parametric Study - Strip Length

An empirical analysis of the length of the parasitic strips near the radiating edges of a microstrip antenna has been carried out in [6]. It was found that the strip length affected the transition region (frequency region where surface waves change to become leaky waves). However, it is mentioned in Section 2.2 that the length of the strips

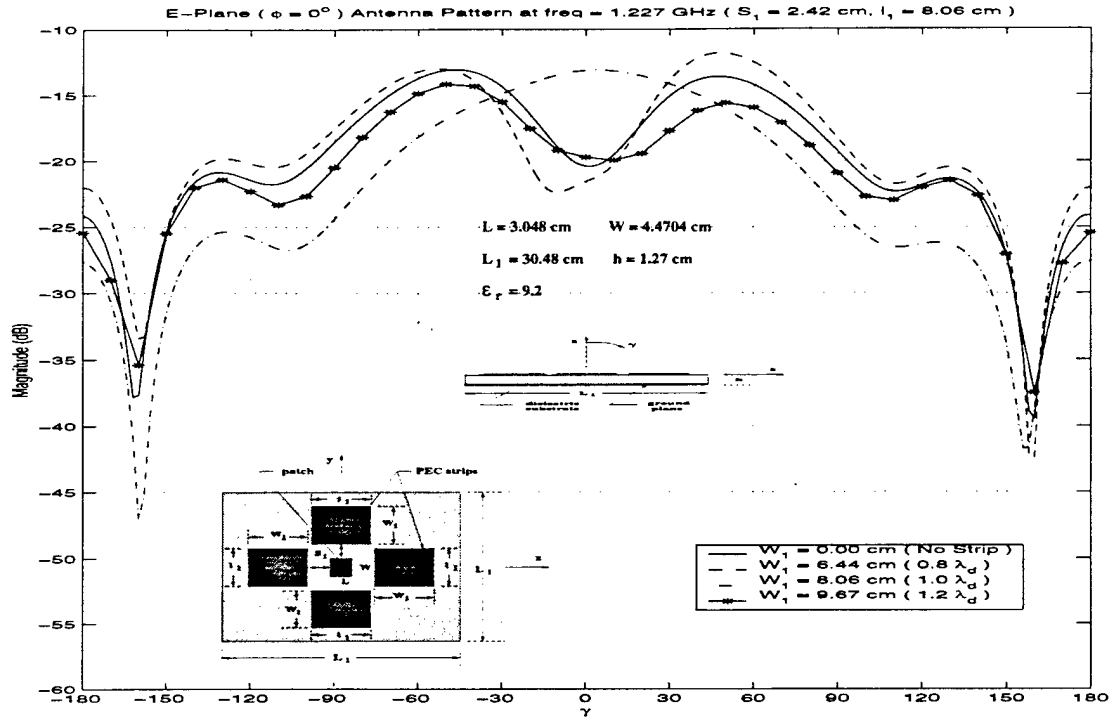


Figure 2.1: Parametric Study - Strip Width: four-strip antenna E-plane pattern with $S_1 = 0.3\lambda_d$, $l_1 = 1.0\lambda_d$ and W_1 varies from 0.8 to $1.2\lambda_d$

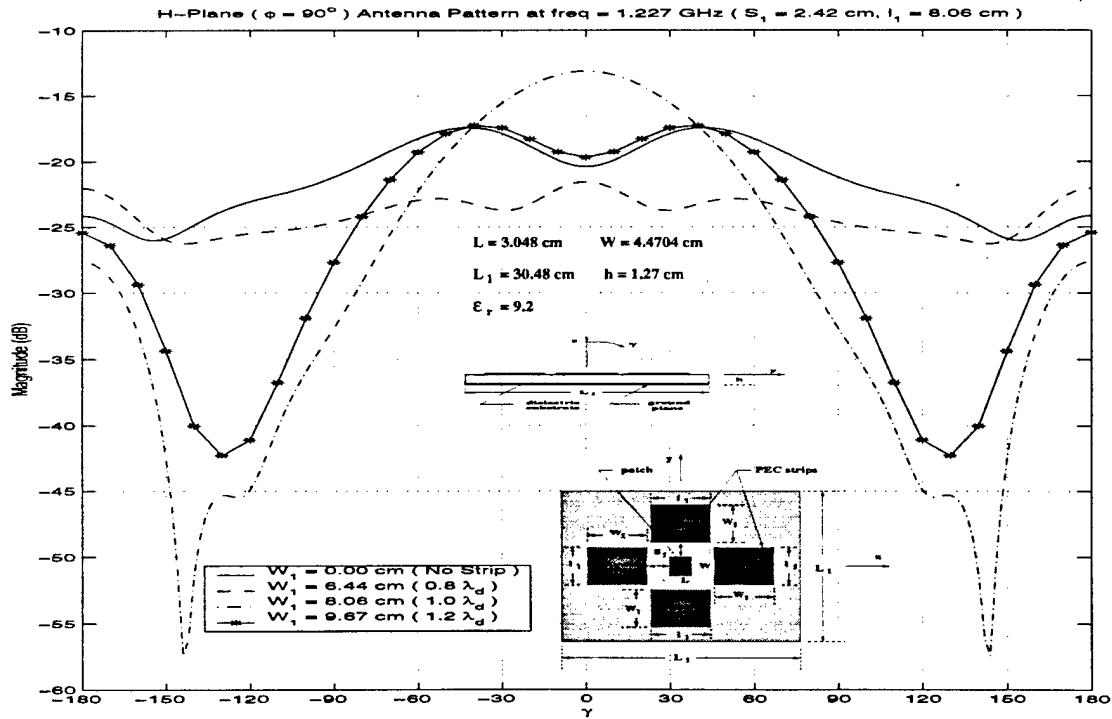


Figure 2.2: Parametric Study - Strip Width: four-strip antenna H-plane pattern with $S_1 = 0.3\lambda_d$, $l_1 = 1.0\lambda_d$ and W_1 varies from 0.8 to $1.2\lambda_d$

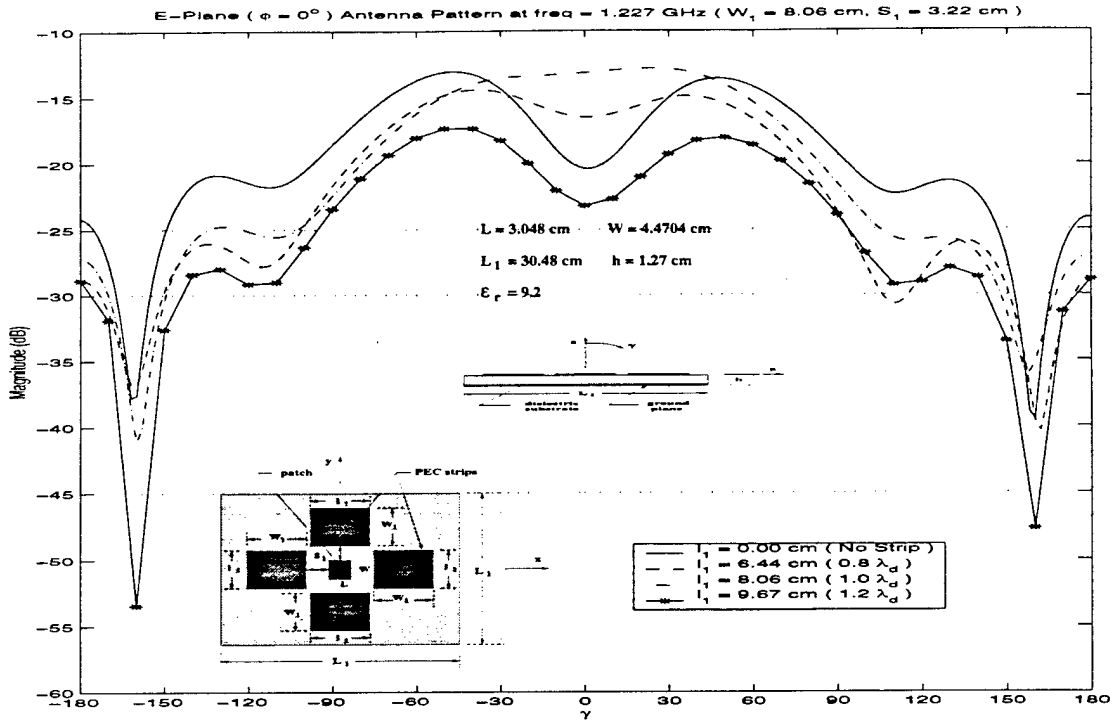


Figure 2.3: Parametric Study - Strip Length: four-strip antenna E-plane pattern with $S_1 = 0.4\lambda_d$, $W_1 = 1.0\lambda_d$ and l_1 varies from 0.8 to $1.2\lambda_d$

cannot be arbitrarily extended in the four-strip case. Since the length and the width of the strips are comparative in magnitude, it is not easy to isolate the effect caused by each of these two strip parameters. This point becomes clear when comparing Figures 2.1 and 2.4. Hence, the two parameters must be designed together, making the design procedure more complicated.

2.4 Parametric Study - Strip Separation

In this section, the effect of the separation of the four strips (from the patch edges) on the far-zone field behavior of the antenna is studied. It can be seen from Figures 2.5 and 2.6 that the antenna patterns do not change significantly when the separation is greater than approximately $0.2\lambda_d$. This is consistent with the two-strip case. Note that the E-plane pattern for the $S_1 = 0.2\lambda_d$ case is different from the other two cases where the edge to strip separation is larger. This effect can be understood by keeping

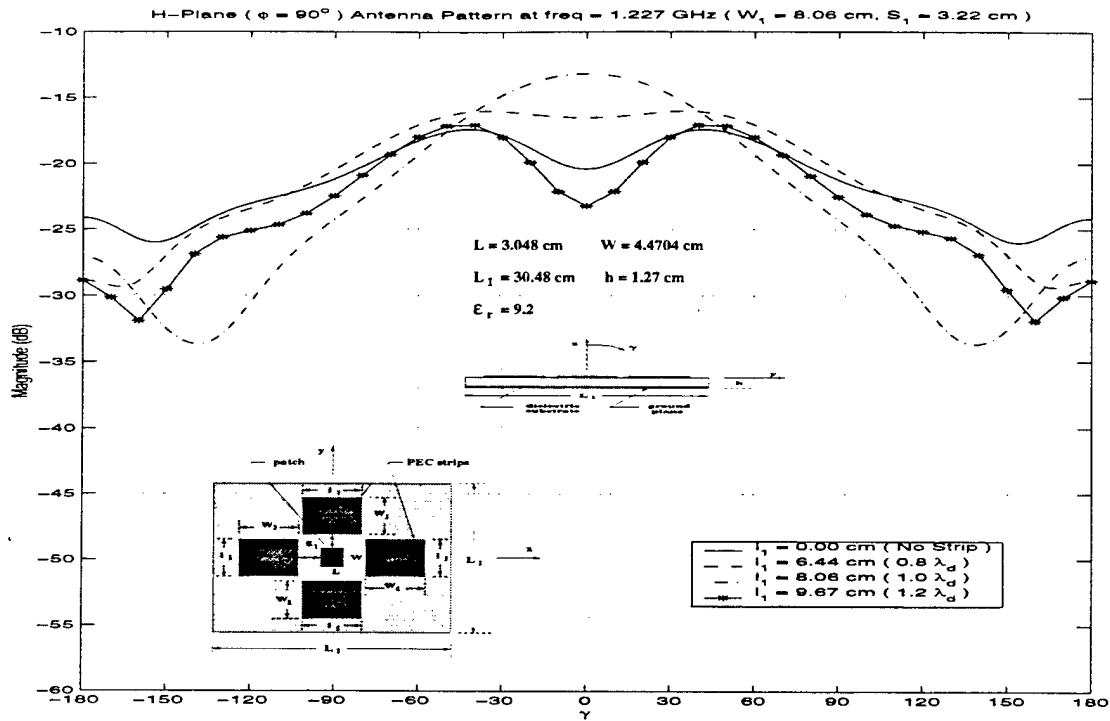


Figure 2.4: Parametric Study - Strip Length: four-strip antenna H-plane pattern with $S_1 = 0.4\lambda_d$, $W_1 = 1.0\lambda_d$ and l_1 varies from 0.8 to $1.2\lambda_d$

in mind that the strips are strongly coupled with the patch antenna, and hence, have a much stronger effect on the field behavior.

2.5 Reconfigurable Antenna Element

In this section, two design examples are presented to illustrate the application of the present scheme in the design of a reconfigurable antenna microstrip element. The design procedure consists of a number of steps which are listed below. The first step is to design four metal strips such that the resultant radiation pattern is significantly modified from the original pattern (without strips). This implies that we are scattering a significant portion of the surface waves. This scatter energy can then be used to modify the pattern in an adaptive fashion. The next step is to divide the metallic strips into smaller pieces and connect them with switches. The switches can be diodes, transistor or RF MEMS. As mentioned before, in this study we are assuming the switches are ideal and are modeled by thin wires when they are

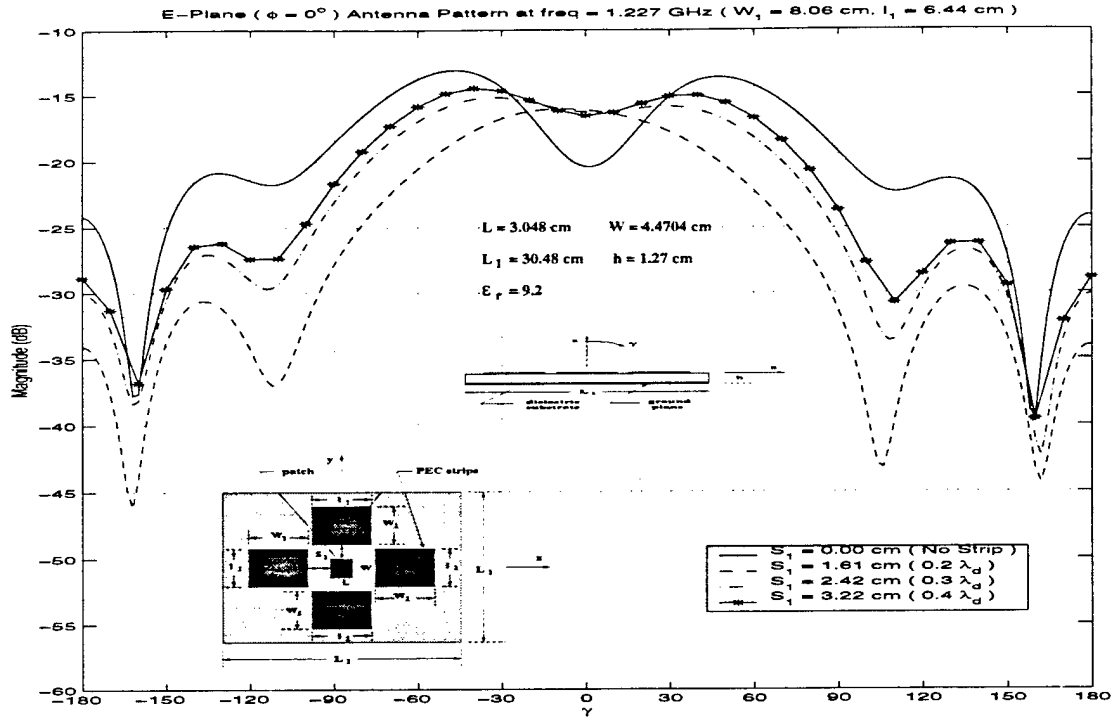


Figure 2.5: Parametric Study - Strip Separation: four-strip antenna E-plane pattern with $l_1 = 0.8\lambda_d$, $W_1 = 1.0\lambda_d$ and S_1 varies from 0.2 to $0.4\lambda_d$

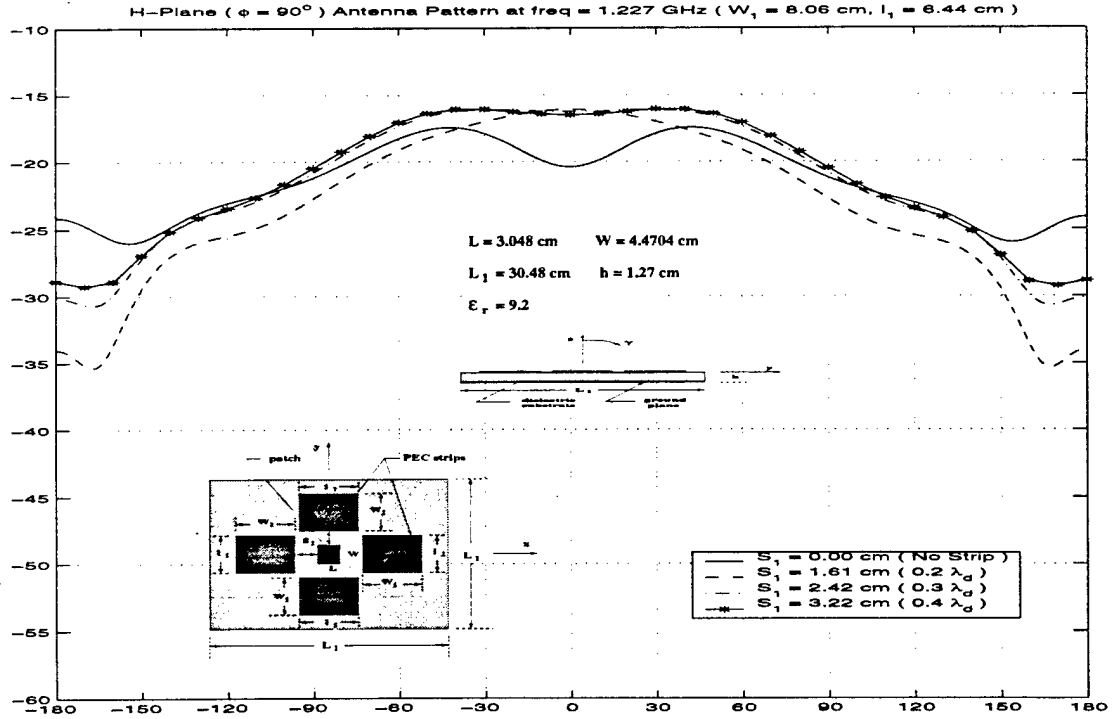


Figure 2.6: Parametric Study - Strip Separation: four-strip antenna H-plane pattern with $l_1 = 0.8\lambda_d$, $W_1 = 1.0\lambda_d$ and S_1 varies from 0.2 to $0.4\lambda_d$

in the “on” state. The wires are removed when the switches are on the “off” state. The key to this step is the way in which the strips are divided and the location and number of the switches. At this stage of the research, this is being done by performing parametric studies on the dimensions of the strips.

The final step is to connect the smaller strips back together by turning the switches on. To obtain the same effect between a solid strip without any switches and the same strip divided into several smaller strips connected with switches, the switches have to be spaced at around $0.1\lambda_d$. This result was obtained in previous studies by numerical experimentation. The radiation pattern of the antenna can then be modified by turning the switches “on” and “off”. In other words, the switches are used to change in real time the dimensions of the parasitic strips.

The first design shows the adaptive feature in the E-plane antenna pattern (Figure 2.7) while the H-plane radiation pattern does not have any significant change (Figure 2.8). The structure on the left in Figure 2.7 represents the case when all the diodes are “on”, while the middle structure in the same figure represents the case when all the diodes are “off”. Note the dramatic change in the radiation patterns between the “on” and “off” stages of the diodes.

The second design shows the adaptive feature in the H-plane antenna pattern (Figure 2.9) while the E-plane radiation pattern does not have any significant change (Figure 2.10).

The above example shows that the radiation pattern in either the E-plane, H-plane, or both, can be significantly modified by the switches placed between the parasitic strips. For an actual application, the strips and switches would have to be designed to achieve the desired change in the pattern.

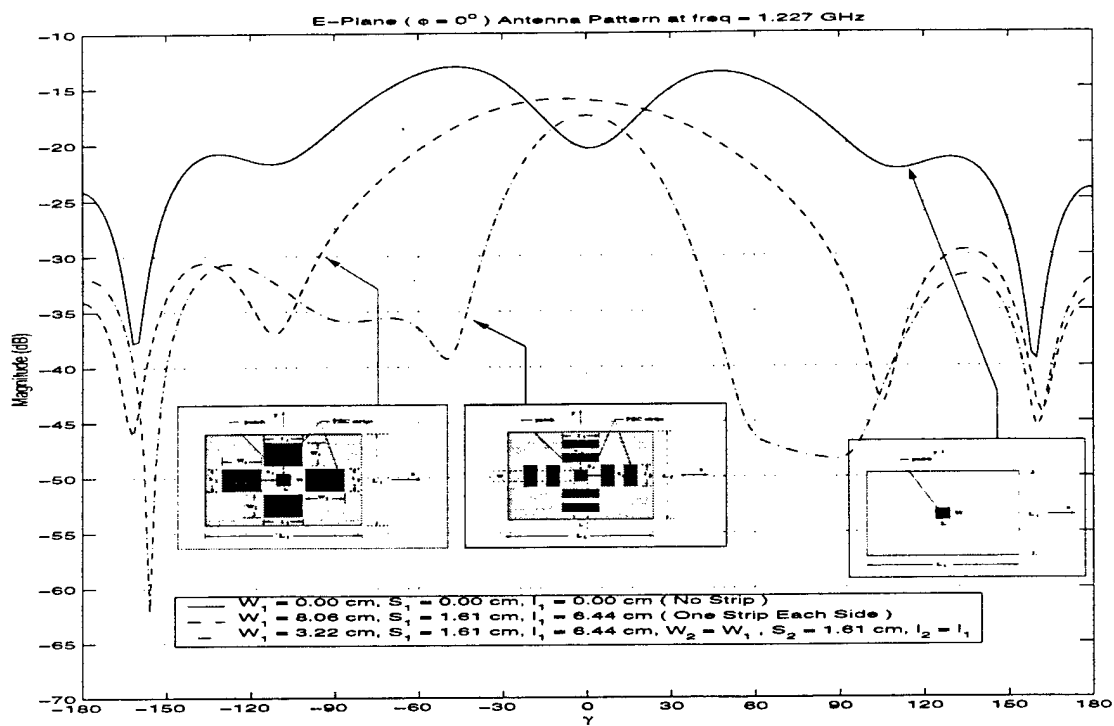


Figure 2.7: Calculated E-plane radiation pattern for design 1

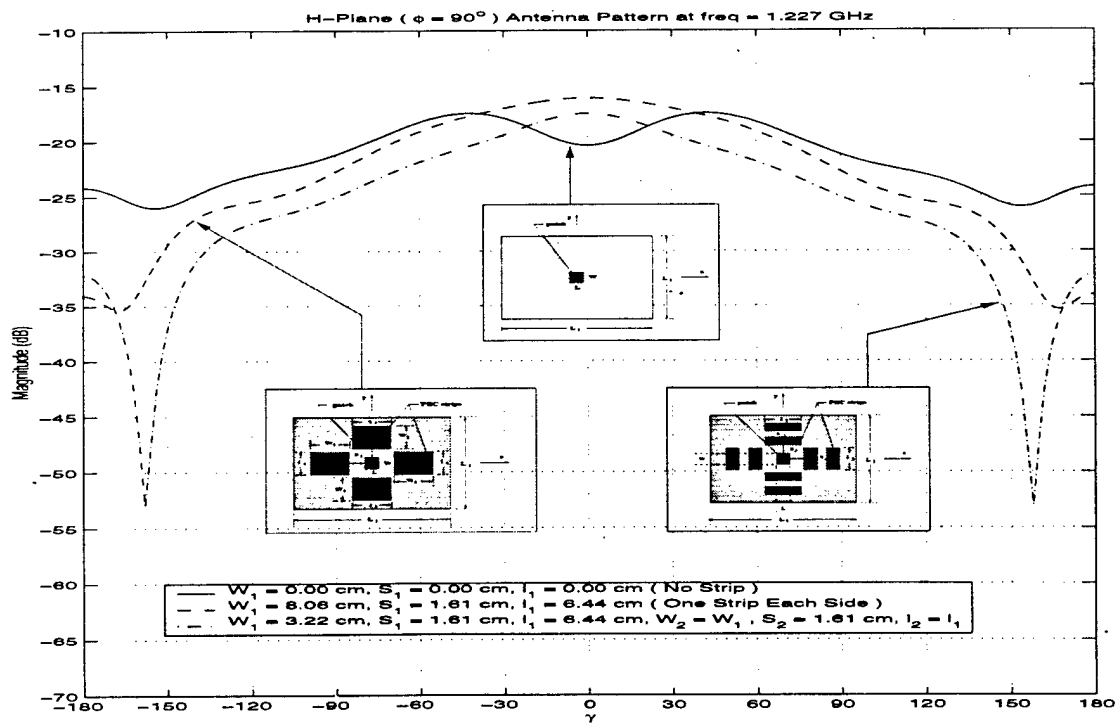


Figure 2.8: Calculated H-plane radiation pattern for design 1

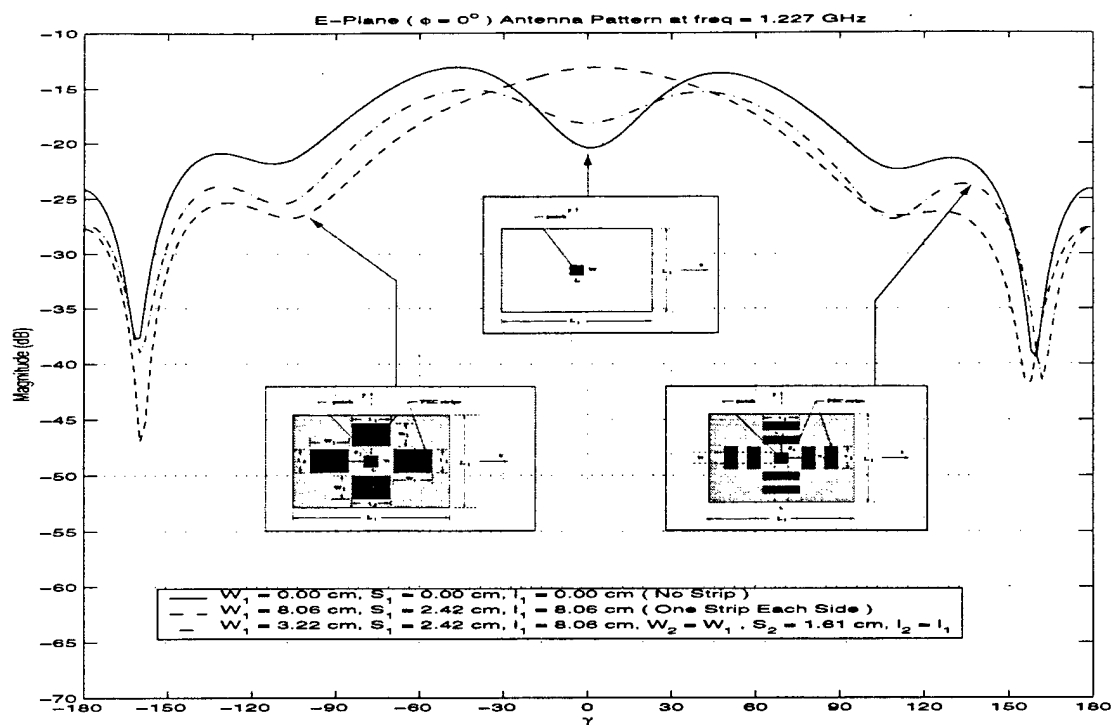


Figure 2.9: Calculated E-plane radiation pattern for design 2

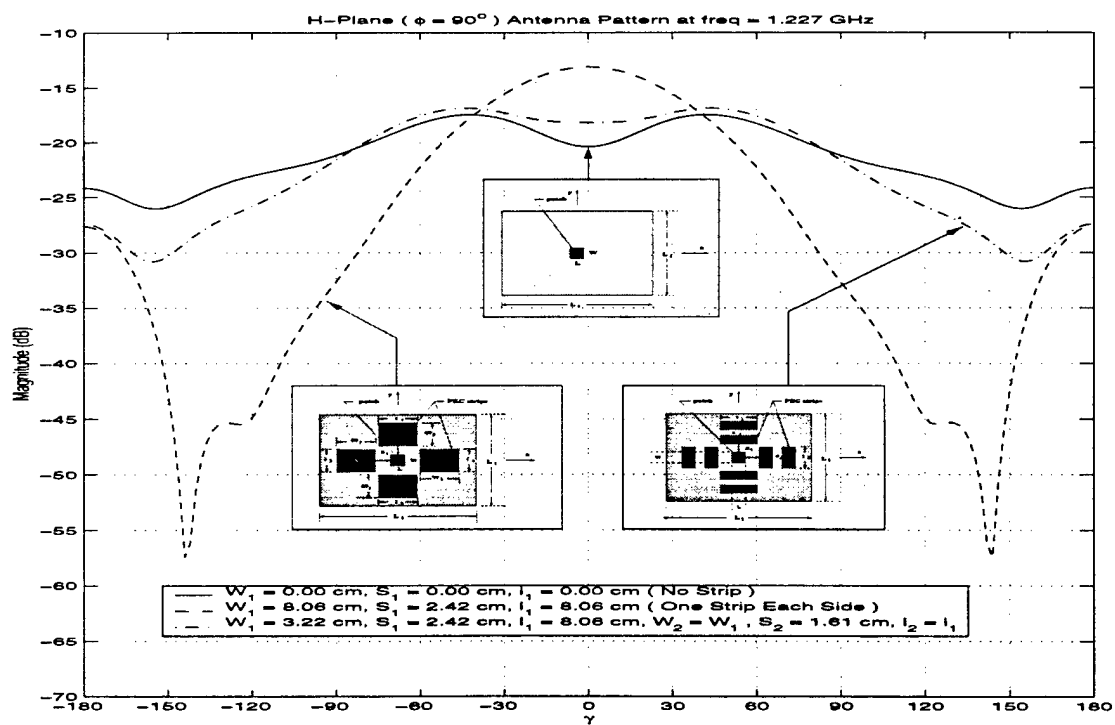


Figure 2.10: Calculated H-plane radiation pattern for design 2

Chapter 3

Circularly Polarized Antenna: Large Ground Plane Case

3.1 Introduction

It is well known that a single probe-feed rectangular microstrip antenna can be designed for circular polarization with an adequate ratio between width and length [10]. In this chapter, a scheme (Figure 1.3) is developed to modify in real time the radiation patterns of such microstrip antenna. The scheme consists in adding metallic rings around the central patch. Due to the presence of the metallic-rings, the field behavior of the antenna changes. The level of change in the radiation patterns of the microstrip antenna is dependent on the width and number of rings and the distance (separation) between the rings and the edges of the patch.

Note that we have initially carried out the analysis at the L2 GPS frequency (1.227 GHz) as a first step. First, two metallic rings connected by switches are designed to provide the adaptive feature at the lower L2 frequency. The same structure will then be tested to see if it can also operate at the L1 frequency. In other words, we are interested in the frequency bandwidth the parasitic rings.

3.2 Parametric Study - Ring Width

In the two and four-strip cases, the width of the strips is the most critical parameter in determining the antenna pattern behavior on a linearly polarized patch antenna.

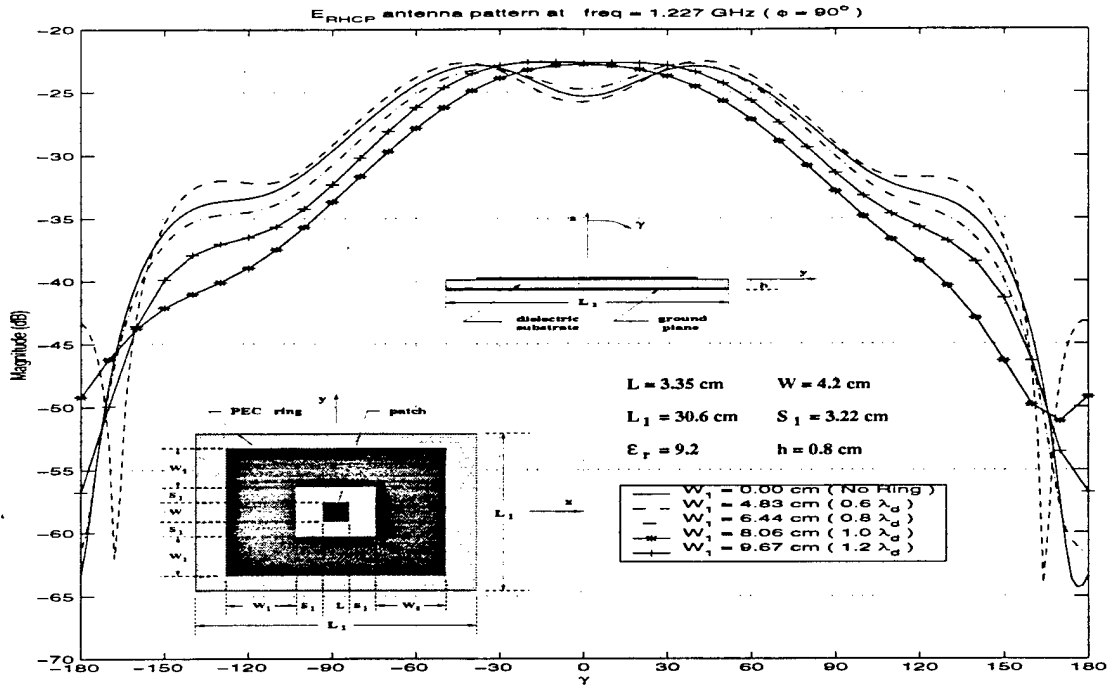


Figure 3.1: Parametric Study - Ring Width: - E_{RHCP} antenna pattern in $\phi = \pm 90^\circ$ plane with $S_1 = 0.4 \lambda_d$ and W_1 varies from 0.6 to $1.2 \lambda_d$

This is also true for circularly polarized antennas, namely, the width of the metal ring has the most significant effect on the overall antenna performance.

When the ring width is electrically small, the ring does not have any significant effect on the microstrip antenna. The resultant antenna pattern has similar "shape" as the antenna pattern without the ring as shown in Figure 3.1 where the pattern is taken in the $\phi = \pm 90^\circ$ plane. When the width of the metallic-ring increases, the resultant antenna pattern has a "flat-top" in the broadside direction and becomes more directive. Thus the ring width has similar effect on the antenna as the two-strip case described in [6]. While the E_{RHCP} is changed due to the variation of the ring width, the cross polarized field (E_{LHCP}) remains small as shown in Figure 3.2.

The antenna patterns in the ($\phi = 0^\circ - 180^\circ$) plane are also shown in Figures 3.3 and 3.4. Due to the symmetry of the structure, it can be seen that the metallic-ring width has the same effect on the other plane as well. However, the antenna patterns are not as symmetry as one may expect. This is because the feed point is in the

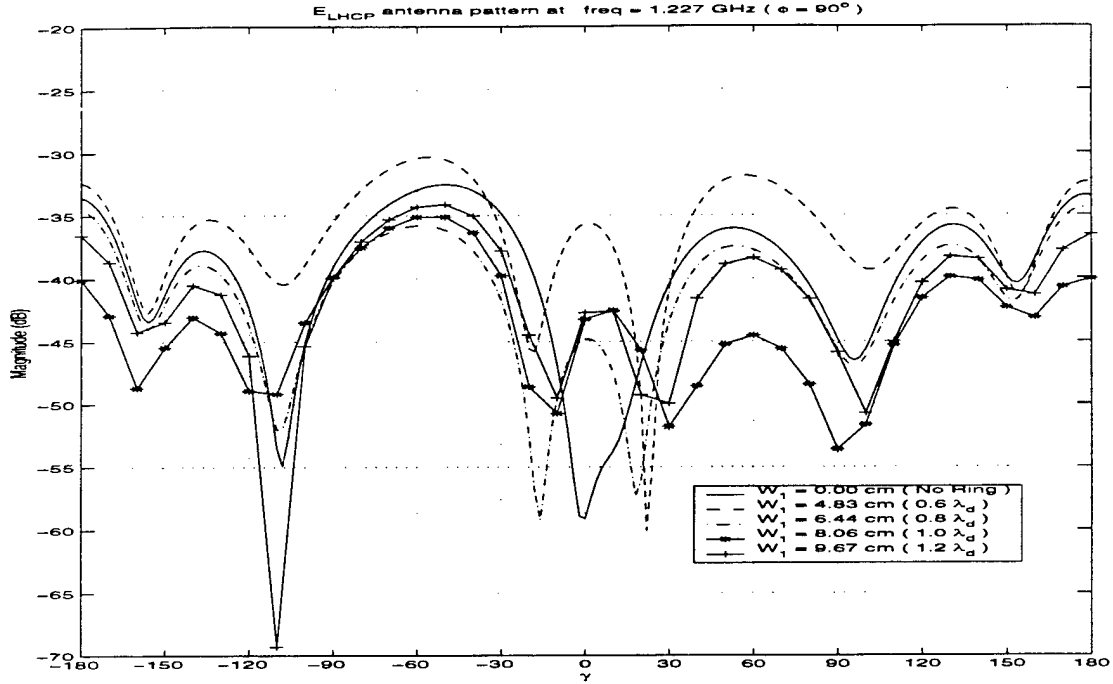


Figure 3.2: Parametric Study - Ring Width: - E_{LHCP} antenna pattern in $\phi = \pm 90^\circ$ plane with $S_1 = 0.4 \lambda_d$ and W_1 varies from 0.6 to $1.2 \lambda_d$

neighborhood of the diagonal, near a corner of the microstrip antenna. Therefore, the probe effect is slightly different in the two planes.

3.3 Parametric Study - Ring Separation

The far-zone field behavior as a function of the separation of the metal-ring from the edge of the circularly polarized patch is briefly discussed in this section. From Figures 3.5- 3.6, it can be observed that varying the separation between the metallic ring and antenna does not cause a significant change in the antenna pattern once the separation exceeds approximately $0.2\lambda_d$. Similar behavior was also observed in previous cases.

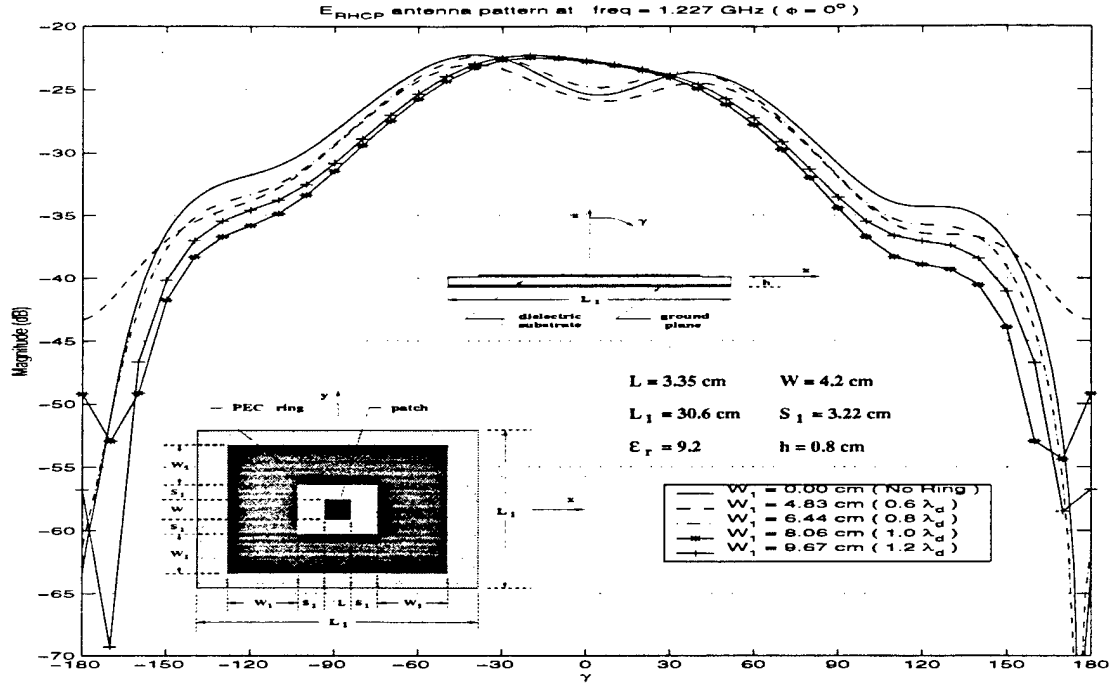


Figure 3.3: Parametric Study - Ring Width: - E_{RHCP} antenna pattern in $\phi = 0^\circ - 180^\circ$ plane with $S_1 = 0.4 \lambda_d$ and W_1 varies from 0.6 to $1.2 \lambda_d$

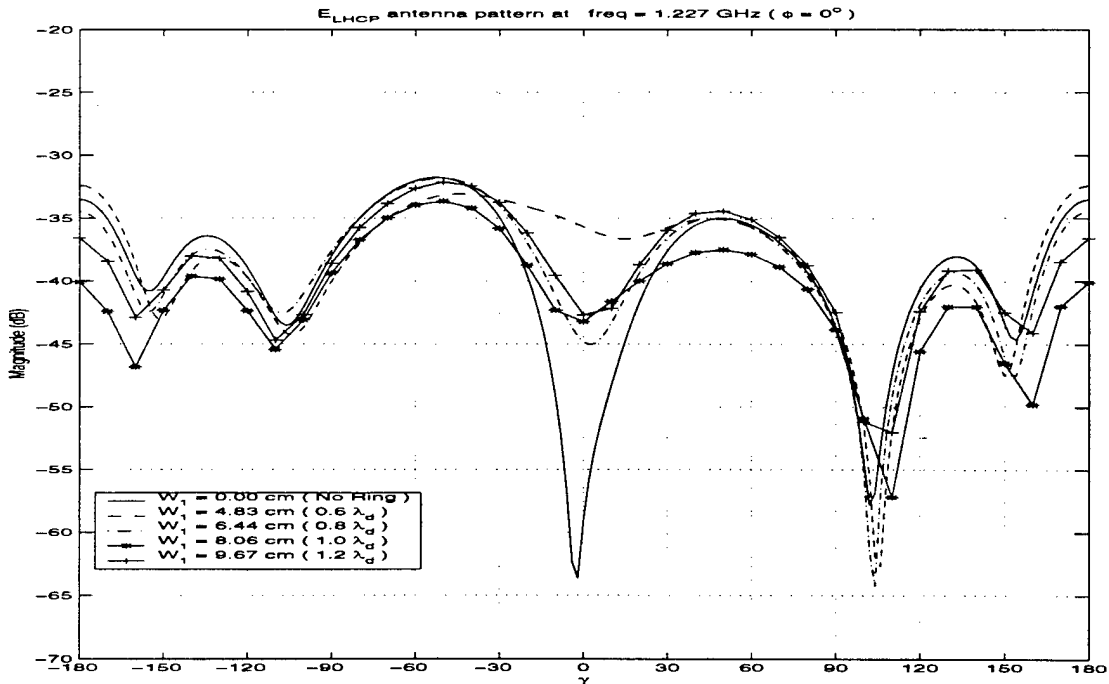


Figure 3.4: Parametric Study - Ring Width: - E_{LHCP} antenna pattern in $\phi = 0^\circ - 180^\circ$ plane with $S_1 = 0.4 \lambda_d$ and W_1 varies from 0.6 to $1.2 \lambda_d$

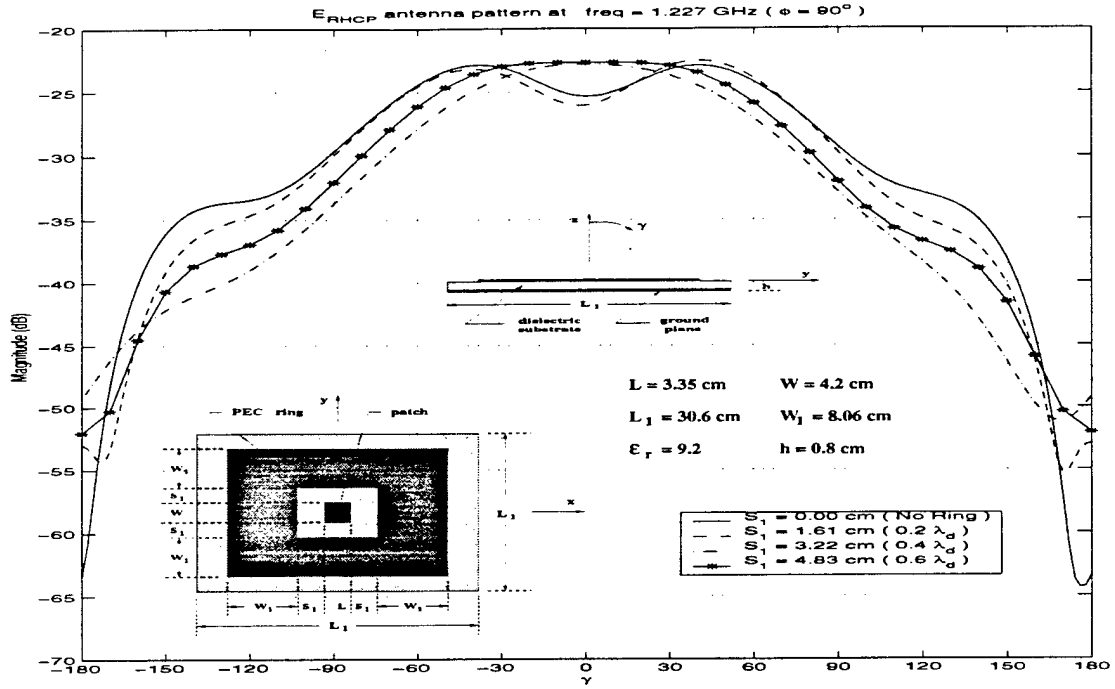


Figure 3.5: Parametric Study - Ring Separation: - E_{RHCP} antenna pattern in $\phi = \pm 90^\circ$ plane with $W_1 = 1.0 \lambda_d$ and S_1 varies from 0.2 to $0.6 \lambda_d$

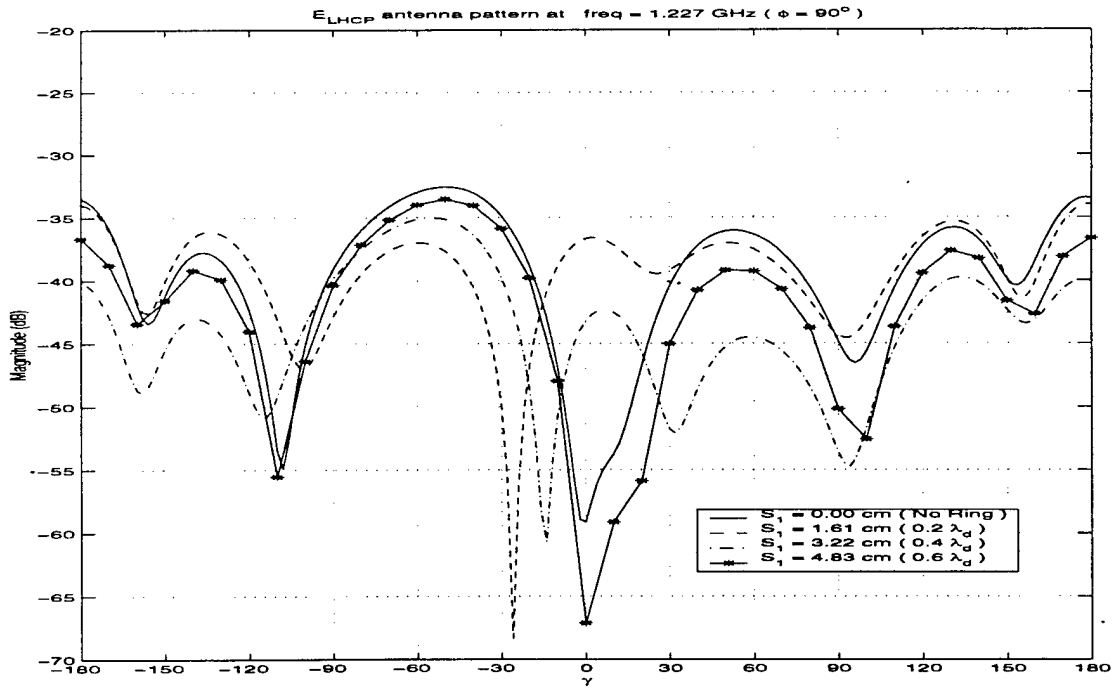


Figure 3.6: Parametric Study - Ring Separation: - E_{LHCP} antenna pattern in $\phi = \pm 90^\circ$ plane with $W_1 = 1.0 \lambda_d$ and S_1 varies from 0.2 to $0.6 \lambda_d$

3.4 Reconfigurable Antenna Element: L2 GPS Frequency

In this section, an example is presented to illustrate the application of the adaptive scheme to a circularly polarized microstrip element. The design procedure is the same as the one mentioned previously for the two and four-strip cases (Section 2.5), namely, the metallic ring is divided into two or more rings and connected with switches. However, there is an important difference from previous cases, namely, the microstrip antenna used here is feed by two probes instead of one. The reason for using two probes is to obtain a more symmetric pattern in terms of the azimuthal angle. Unless otherwise mentioned, all the results in the rest of this report are for a two-probe CP microstrip antenna.

In the following examples the only operating states of the ring to be considered are when all the switches are "on" and all the switches are "off". Obviously, there are many other operating states corresponding to the situation when only a portion of the switches are "on" and the rest are "off", however, they will not be considered in this report. The large single ring represents the case when all the switches are "on", while the two concentric smaller rings represent the case when all the switches are "off". It should be kept in mind that the position and number of switches has not been optimized. The results presented here are only to demonstrate the feasibility of this scheme. Note that the ring parameters in the following examples are defined with respect to the origin of the coordinate system and are independent of the size of the microstrip antenna. This is contrast to all the previous examples where the ring dimensions were defined with respect to the microstrip patch antenna. From Figures 3.7 and 3.8, we notice that while the right-hand circularly polarized pattern changes between the two cases described above, the cross polarized component (left-hand circularly polarized pattern) remains at a fairly low level. For completeness, radiation patterns for the patch antenna by itself are also included in Figures 3.7-3.8. It is clear that the metallic-ring structure has the ability to change the beamwidth

of the E_{RHCP} pattern while keeping the E_{LHCP} pattern at a low level (approximately 10 dB lower at broadside with respect to the E_{RHCP} component).

3.5 Reconfigurable Antenna at L1 GPS Frequency

The first goal of this section is to assess the performance of the ring structure introduced in the previous section for operation at the higher L1 frequency. Since the circularly polarized microstrip antenna at 1.575 GHz is smaller than the antenna designed to operate at 1.227 GHz, the separation between the ring and the antenna is different for the case being considered in this section.

The patterns of the RHCP and LHCP components at the higher frequency (L1) are depicted in Figures 3.9-3.9. Notice that the beamwidth of the RHCP component does not change very much between the two operating states of the parasitic ring when used at the L1 frequency. To have a significant effect on the pattern, it is necessary to modify the placement of the switches and the widths of the two metallic rings. Increasing S_3 and S_4 , while decreasing W_1 and W_2 to keep the overall width of the structure the same yields the patterns depicted in Figures 3.11-3.12. It can be observed that the beamwidth of the RHCP component can be modified, especially around $\pm 90^\circ$ where a change of around 5 dB is obtained. The cross-polarized component (LHCP) remains at a lower level, although it increases in magnitude for the two ring case (all switches "off"). This is to be expected because the design has not been optimized.

When this ring structure is applied back to the RHCP microstrip antenna at 1.227 GHz (Figures 3.13-3.14), the change in the main beam pattern of the RHCP component is not the desired one. This indicates that further study is needed to obtain an optimum placement of the switches to be able to control the pattern at L1 and L2 simultaneously.

To conclude, the ability of the metallic-ring structure to control the antenna pattern (E_{RHCP}) is established. The optimal design of the number and placement of the switches that yield a ring able to operate simultaneously at L1 and L2 frequencies requires further study. In the next chapter, a new scheme is presented in the attempt

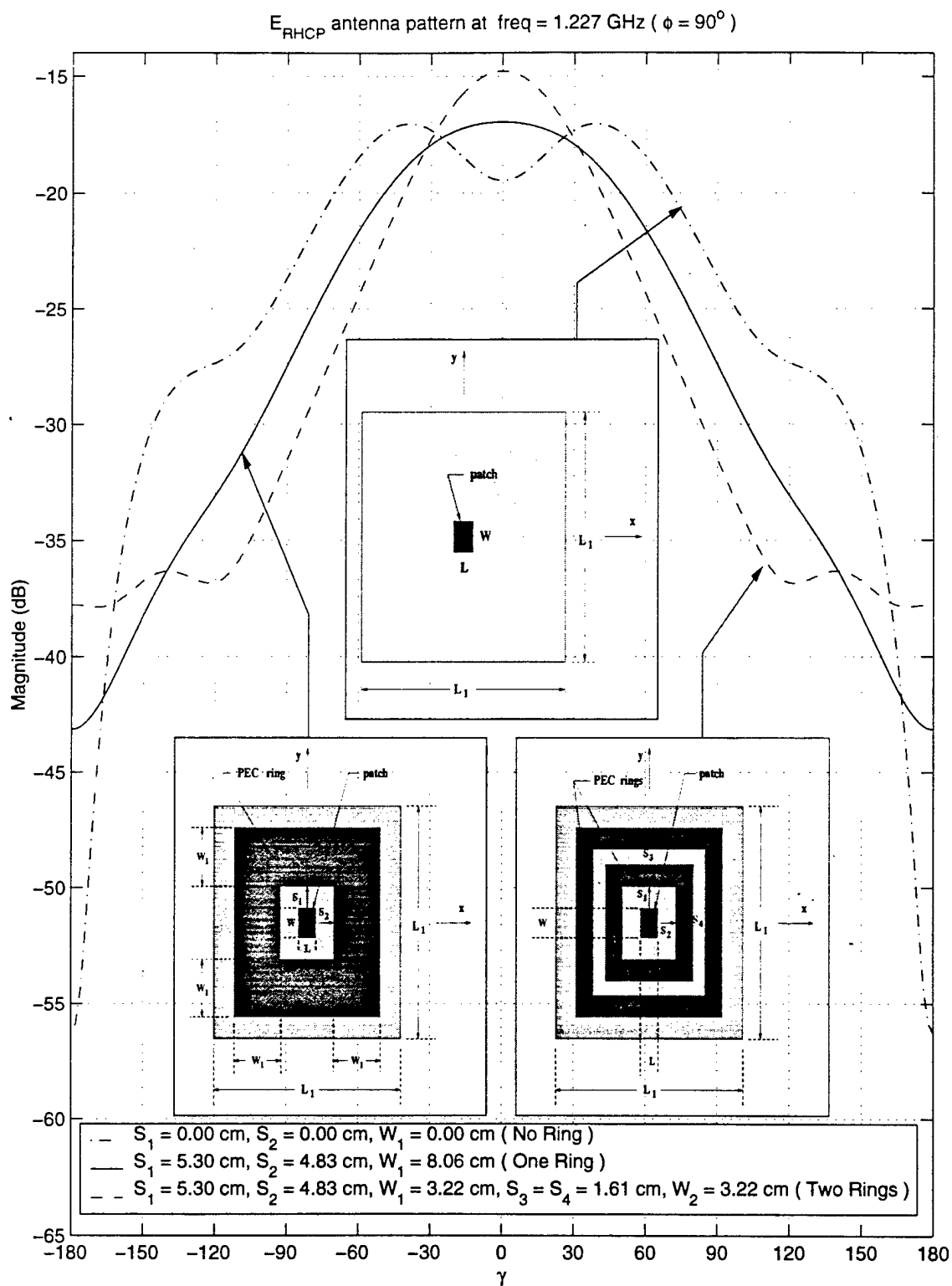


Figure 3.7: Calculated E_{RHCP} antenna pattern at $\phi = 90^\circ$ and $f = 1.227$ GHz for the adaptive circularly polarized patch antenna (Design 1).

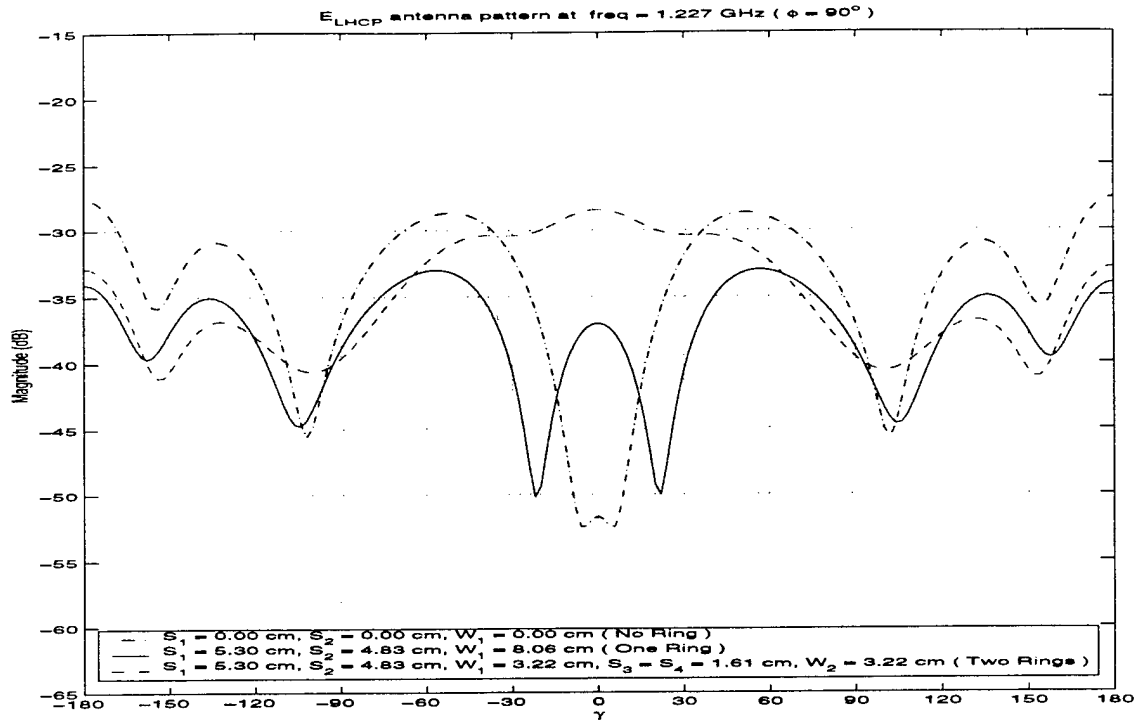


Figure 3.8: Calculated E_{LHCP} antenna pattern in $\phi = \pm 90^\circ$ plane at $f = 1.227$ GHz for the adaptive circularly polarized patch antenna (Design 1).

to improve the dual frequency operation property of the present scheme as well as to reduce the overall size of the antenna.

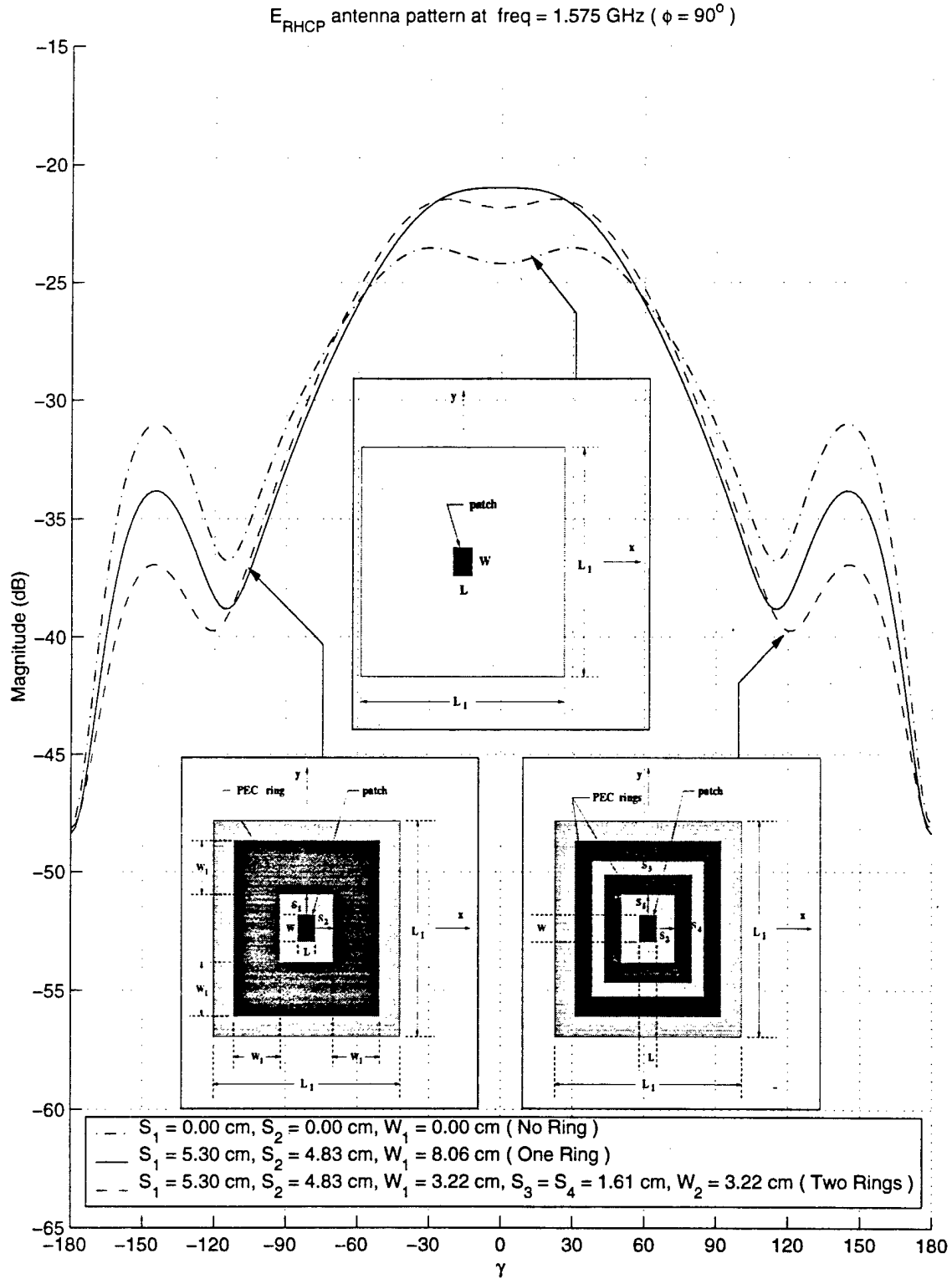


Figure 3.9: Calculated E_{RHCP} antenna pattern in $\phi = \pm 90^\circ$ plane at $f = 1.575$ GHz for the adaptive circularly polarized patch antenna (Design 1).

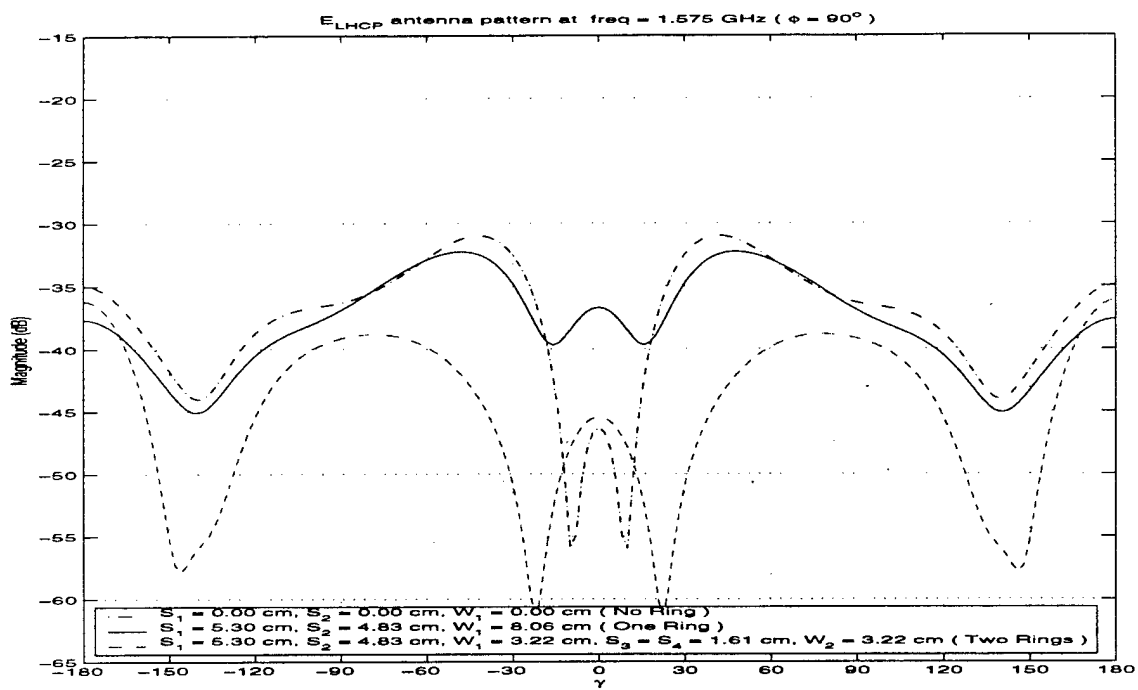


Figure 3.10: Calculated E_{LHCP} antenna pattern in $\phi = \pm 90^\circ$ plane at $f = 1.575$ GHz for the adaptive circularly polarized patch antenna (Design 1).

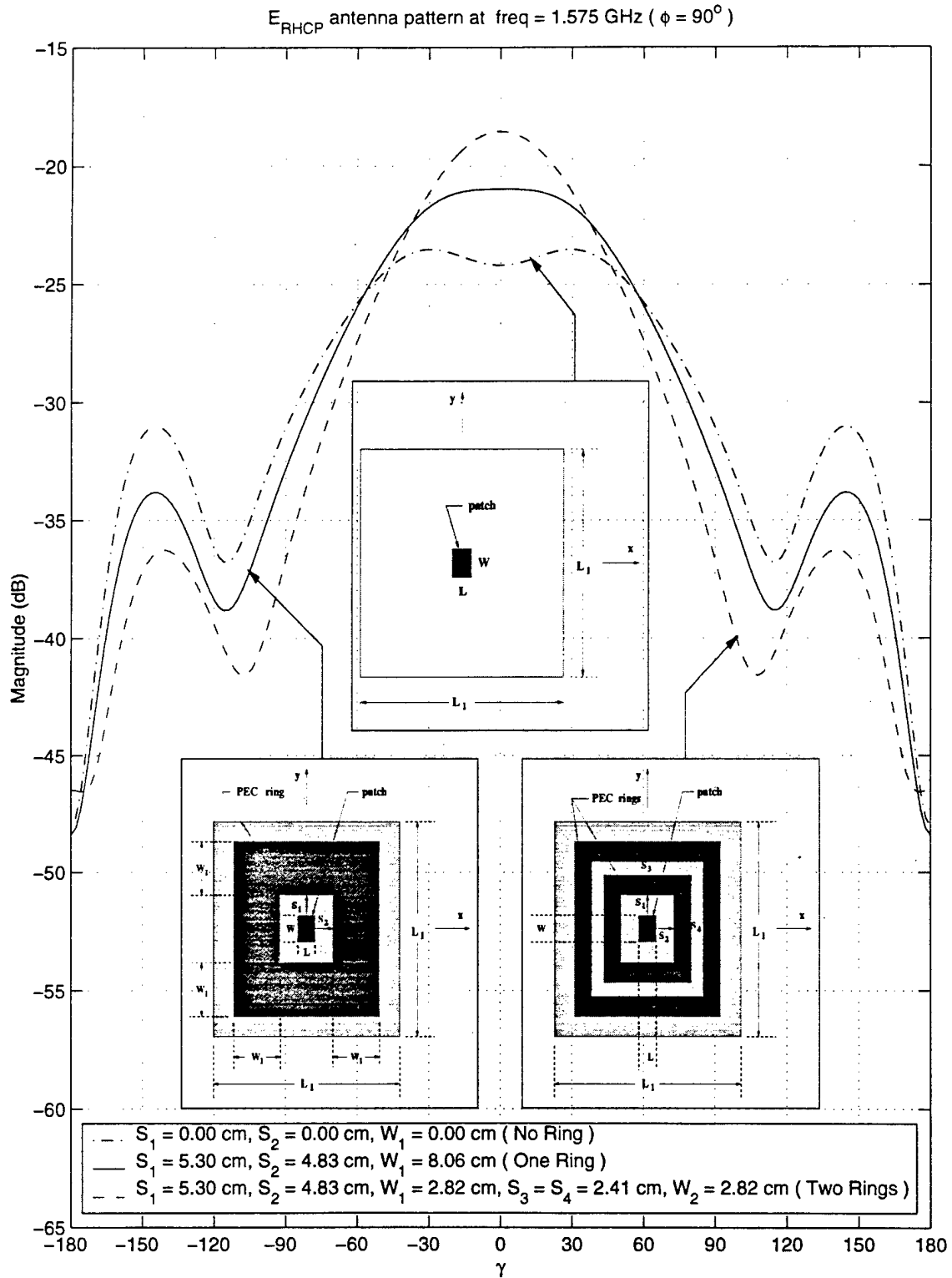


Figure 3.11: Calculated E_{RHCP} antenna pattern in $\phi = \pm 90^\circ$ plane at $f = 1.575$ GHz for the adaptive circularly polarized patch antenna (Design 2).

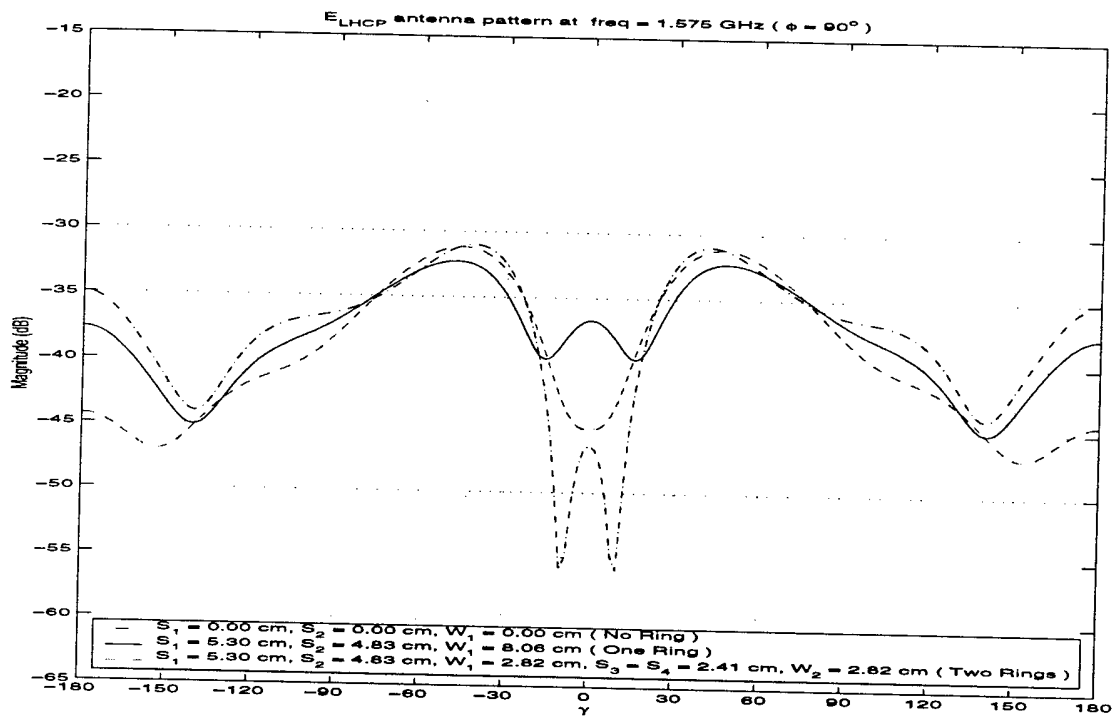


Figure 3.12: Calculated E_{LHCP} antenna pattern in $\phi = \pm 90^\circ$ plane at $f = 1.575$ GHz for the adaptive circularly polarized patch antenna (Design 2).

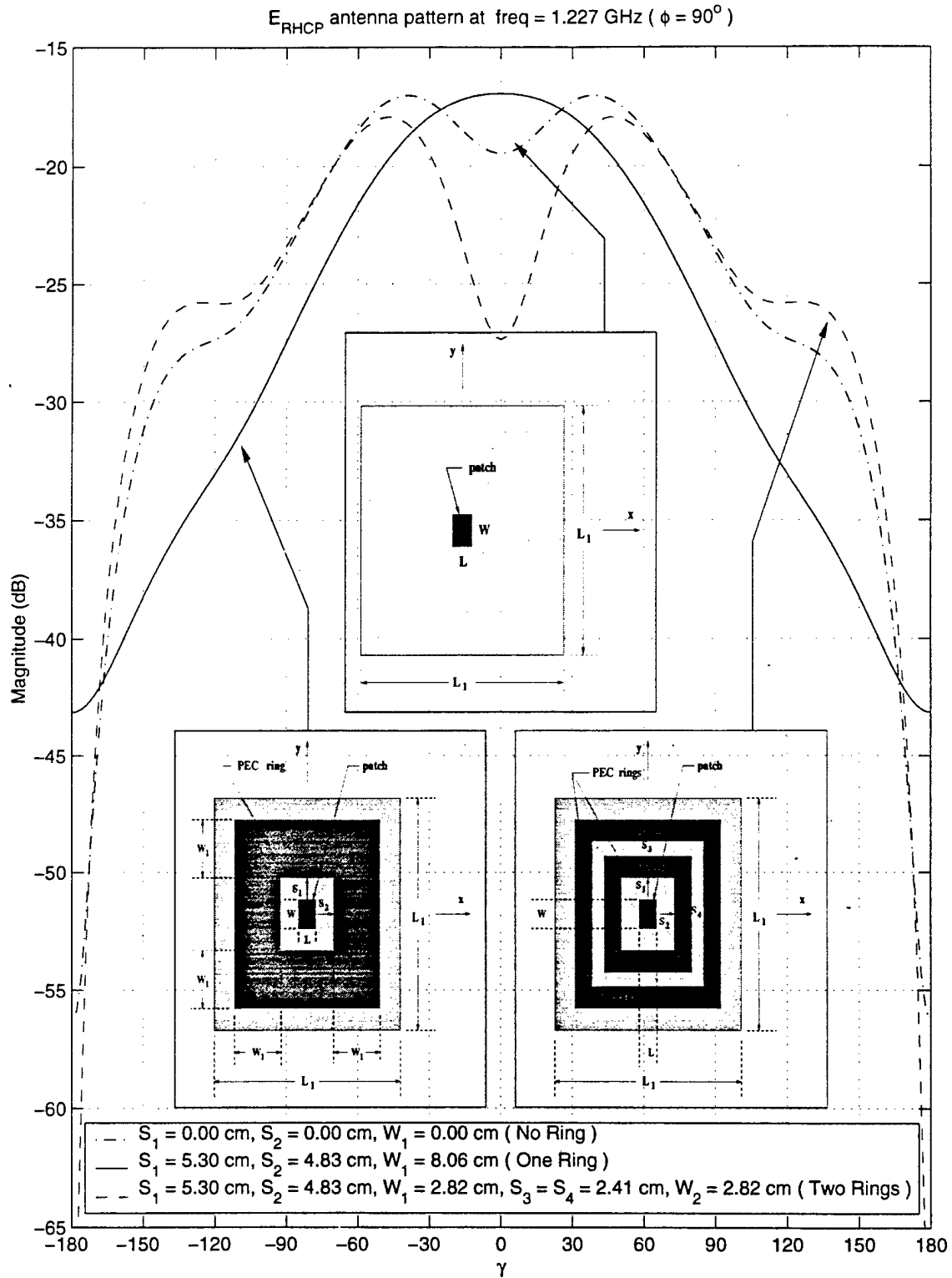


Figure 3.13: Calculated E_{RHCP} antenna pattern in $\phi = \pm 90^\circ$ plane at $f = 1.227 \text{ GHz}$ for the adaptive circularly polarized patch antenna (Design 2).

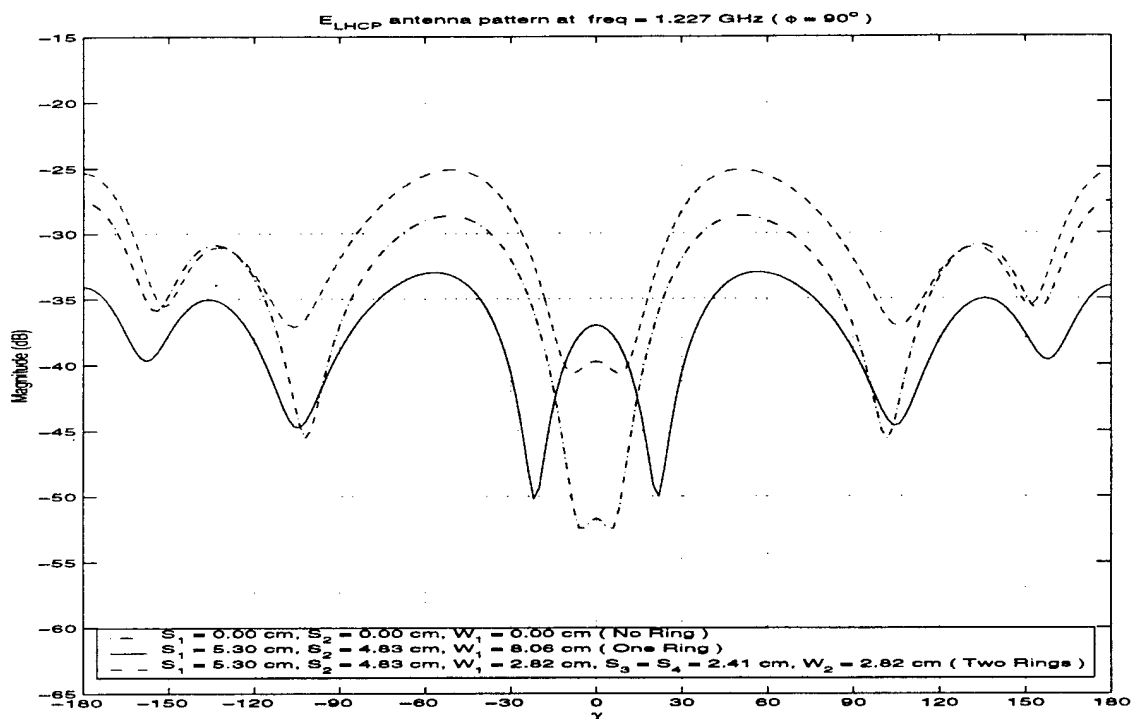


Figure 3.14: Calculated E_{LHCP} antenna pattern in $\phi = \pm 90^\circ$ plane at $f = 1.227$ GHz for the adaptive circularly polarized patch antenna (Design 2).

Chapter 4

Circularly Polarized Antenna: Small Ground Plane Case

4.1 Introduction

In the previous chapter, we presented a circularly polarized reconfigurable planar microstrip antenna. Although the proposed scheme shows the ability to control the beamwidth of the antenna at both GPS frequencies, the overall size of the antenna is large. It also appears that it may be difficult to use the same operating state of the parasitic rings to control both frequencies (L1/L2) at the same time. To overcome the above problems, an alternative configuration is proposed in this chapter.

To improve the previous scheme it is necessary to increase the strength of the surface waves which will result in a smaller metallic ring. The resulting metallic-ring, whose typical width is around $0.1 \lambda_d$ at 1.227 GHz , is shown in Figure 1.4. The important feature of this design is the fact that the ring is larger than the ground plane for the microstrip antenna. Since the ring is fairly thin, it can easily be divided into smaller pieces and connected with switches as depicted in 1.5. The antenna pattern beamwidths can then be modified by controlling the “on” and “off” states of the switches.

This new scheme has two important advantages over previous designs. First of all, the overall size of the antenna, including the rings is smaller than previous designs. Secondly, since the width of the ring is smaller, it is much easier to determine the placement of the switches to simultaneously control the antenna pattern beamwidth

at the two GPS frequencies. Preliminary results of a simple parametric study are presented in the next section followed by examples where various operating states of the ring are studied to determine its effect on the radiation pattern.

4.2 Preliminary Analysis

A parametric study of the present scheme is very complicated. This is true because the performance of the resultant reconfigurable antenna element depends on a large number of parameters (ground plane size, width and diameter of metal ring, horizontal distances between the edges of the ground plane and the inner edges of the metallic ring, etc.). In this section, we perform a preliminary study on the general behavior of the present configuration.

All the adaptive schemes that we presented are based on the idea of changing the surface wave behavior within the dielectric substrate to shape the radiation patterns. Thus, most of these schemes perform well when stronger surface waves are excited. This is especially true for the present scheme. The strength of the surface waves can be increased by decreasing the size of the ground plane such that a portion of the substrate between the antenna and the parasitic ring is without any metallic cover. We can easily understand the advantage of this such a structure by considering a dielectric waveguide with and without a ground plane (see Figures 4.1) [11]. The dielectric waveguide without ground plane supports even and odd $TM_{x,z}$ and $TE_{x,z}$ modes, while the grounded dielectric waveguide only supports odd $TM_{x,z}$ and even $TE_{x,z}$ modes (half the modes of the former waveguide). Thus, it is expected that for the same substrate thickness, the dielectric waveguide without ground plane supports stronger surface waves than the latter waveguide. Keeping this in mind, the ground plane of the microstrip antenna has to be carefully designed to achieve the above waveguide with the proper length and thickness. At the present time, this is done in the computer performing a parametric study to determine the proper dimensions of the ground plane. Figure 4.2 shows radiation patterns as a function of the size of the ground plane. It can be observed that the radiation pattern can be significantly modified by varying the dimensions of the ground plane and the dielectric waveguide.

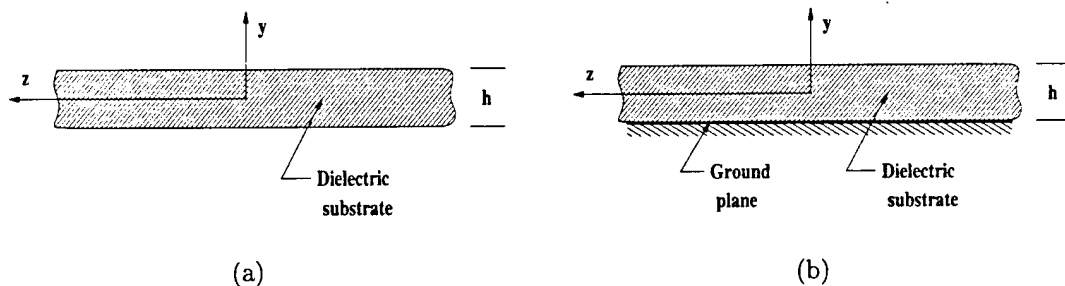


Figure 4.1: Geometry for (a) dielectric slab waveguide without a ground plane and (b) grounded dielectric waveguide

After obtaining a desired ground plane size, the next step is to place a metallic ring on the substrate around the microstrip antenna. By doing so, the characteristics of the surface waves can be modified. The amount of the changes depends on the width of the ring and the horizontal distance between the ring and the outer edge of the ground plane. As mentioned above, it is important to have such a spacing between the two in order for the present scheme to work.

The last step is to design the location and number of switches on the metallic ring such that the resultant antenna element has the ability to modify its pattern beamwidth by controlling the operation of the switches. Of course, there are many different ways that the switches can be placed on the metallic ring, however, due to the small width of the ring, placing the switches along the circumference of the ring appears to be the logical approach. A rigorous approach requires an analysis of the induced current behavior on the ring. Thus, if we wanted to have a large (small) variation in the antenna pattern, then we would place the switches at the positions where there exist current peaks (nulls). However, at the present time, we place the switches by trail and error. An example is given in Figures 4.3- 4.4 for the L2 GPS frequency while Figures 4.5- 4.6 show results for the higher L1 GPS frequency. From these figures, we can see that a drastic change in the antenna pattern occurs with only small changes in the placement of the switches on the metallic-ring structure. Note that it is important to examine the behavior at both GPS frequencies for dual frequency operation.

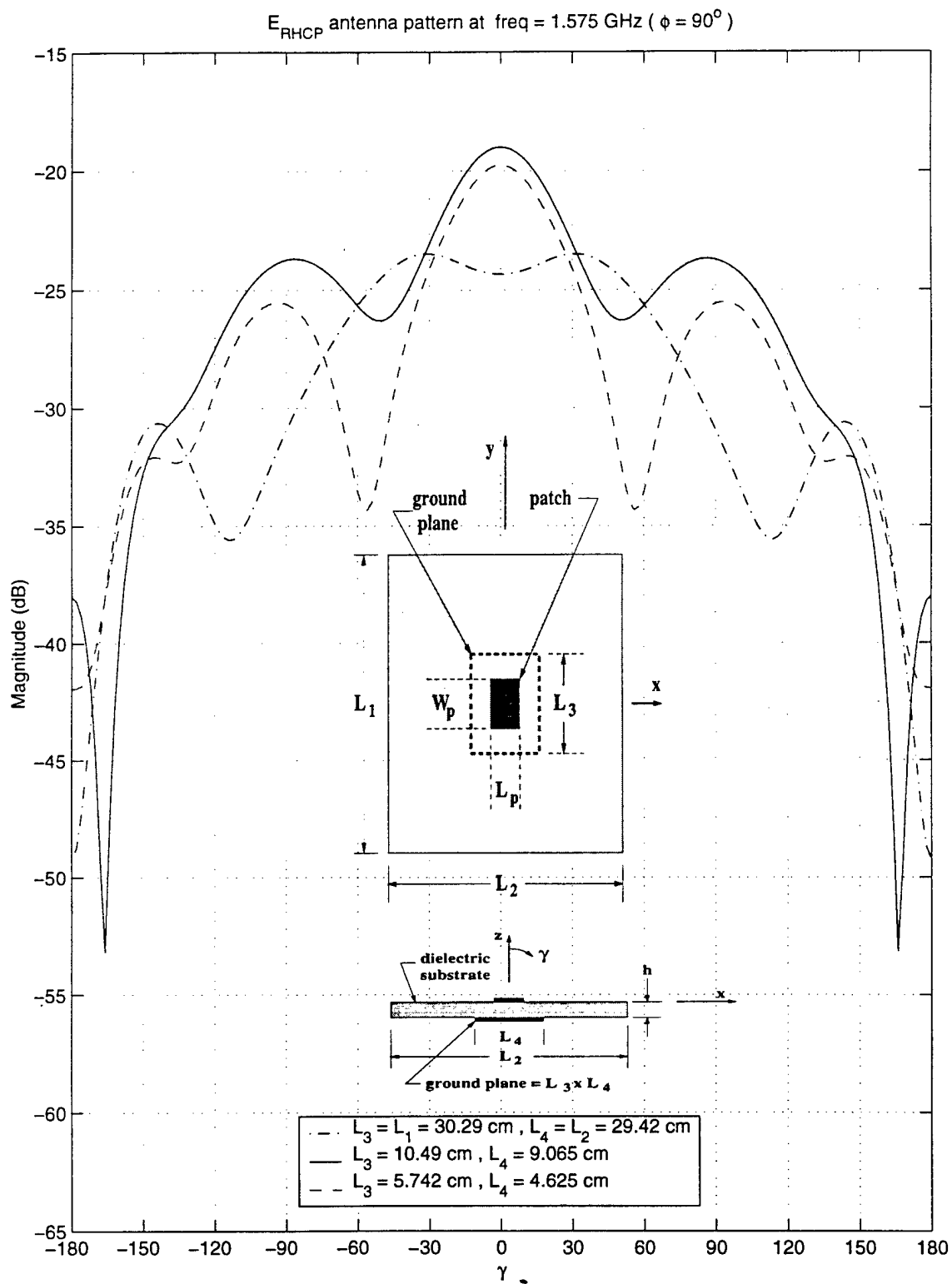


Figure 4.2: Preliminary analysis on the effect of the ground plane dimensions (L_3 , L_4) on the radiation pattern, L1 band

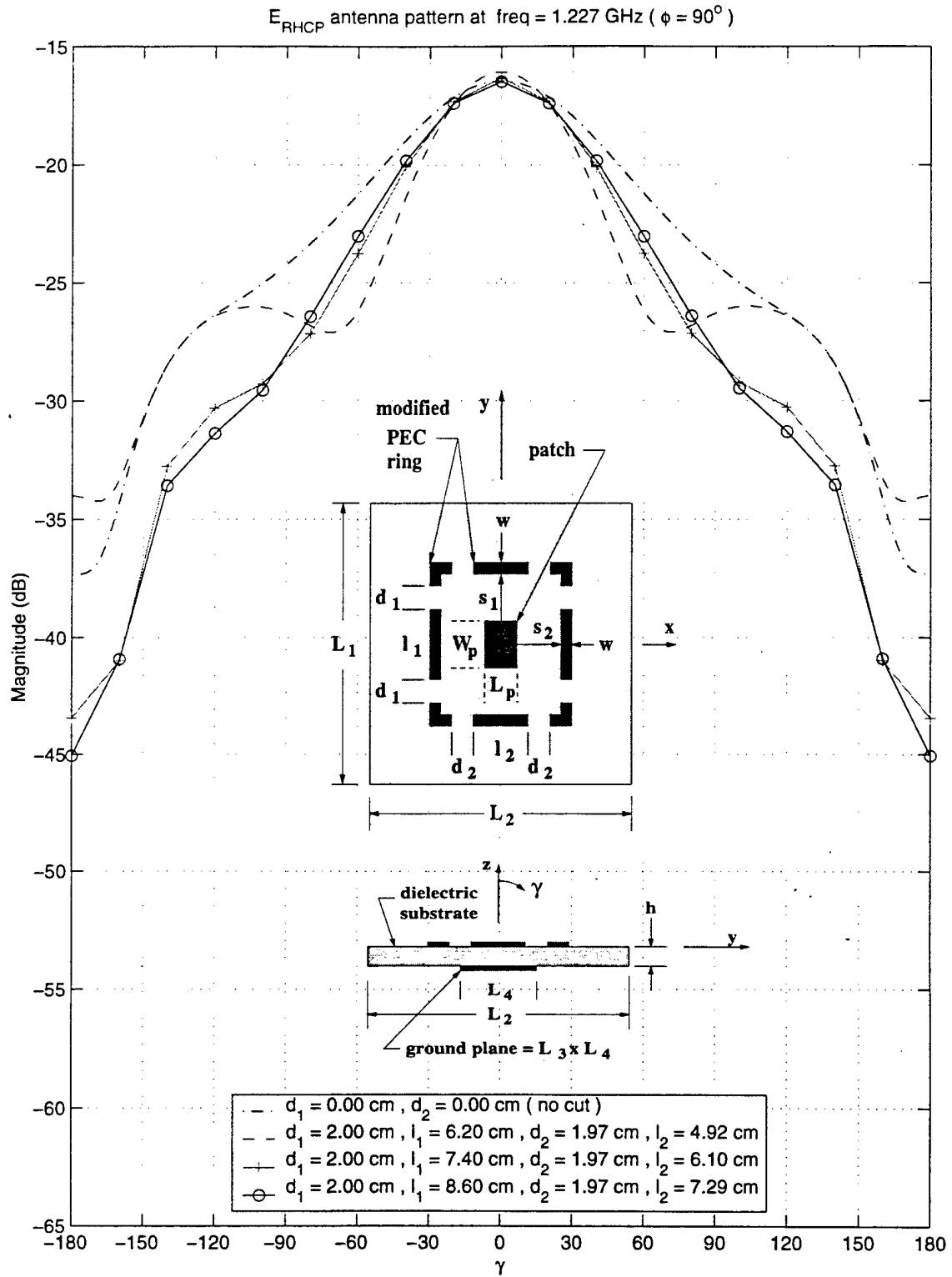


Figure 4.3: Radiation pattern of E_{RHCP} in $\pm 90^\circ$ plane as a function of ring dimensions l_1 and l_2 , L2 band

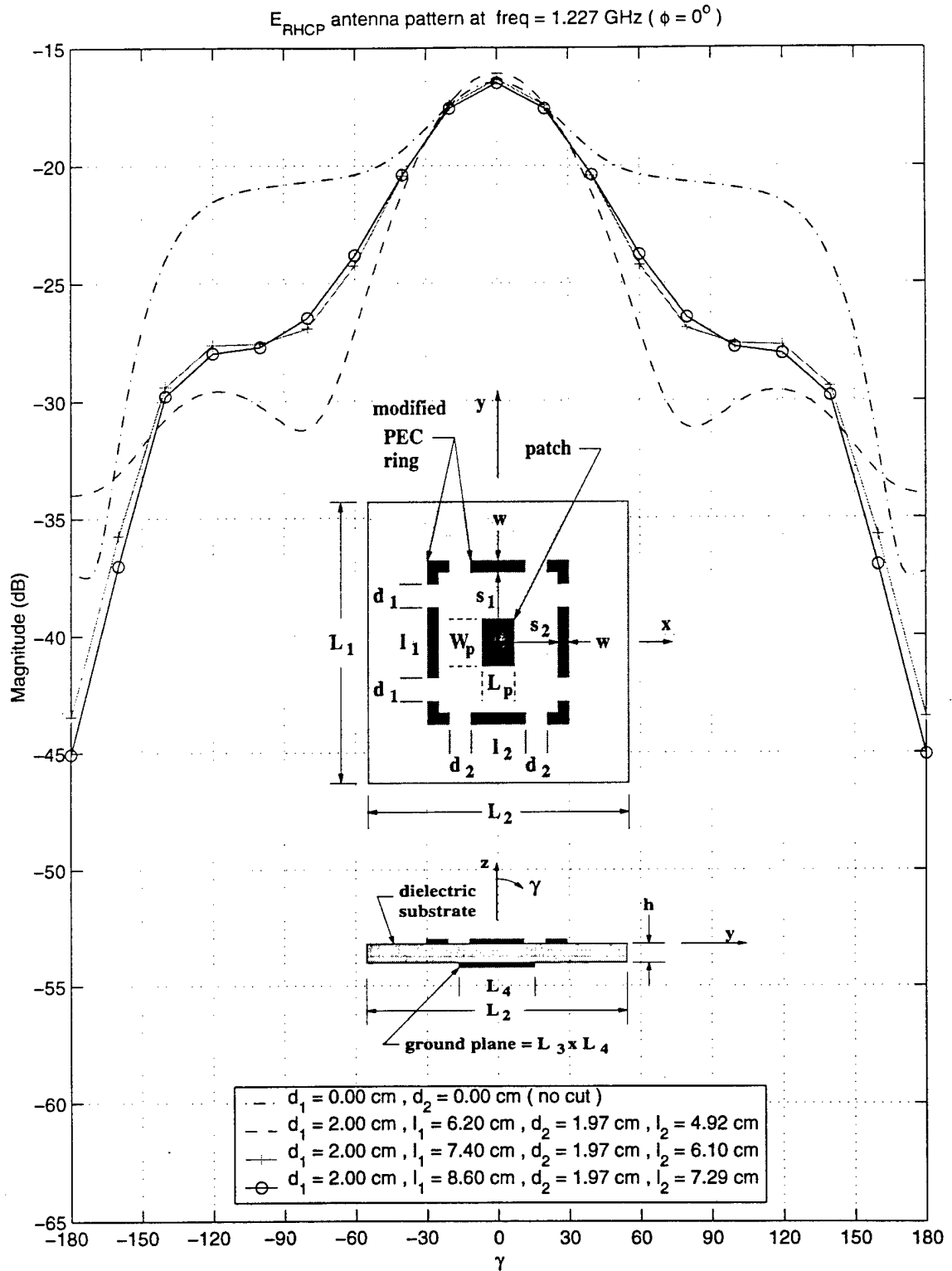


Figure 4.4: Radiation pattern of E_{RHCP} in $0^\circ - 180^\circ$ plane as a function of ring dimensions l_1 and l_2 , L2 band

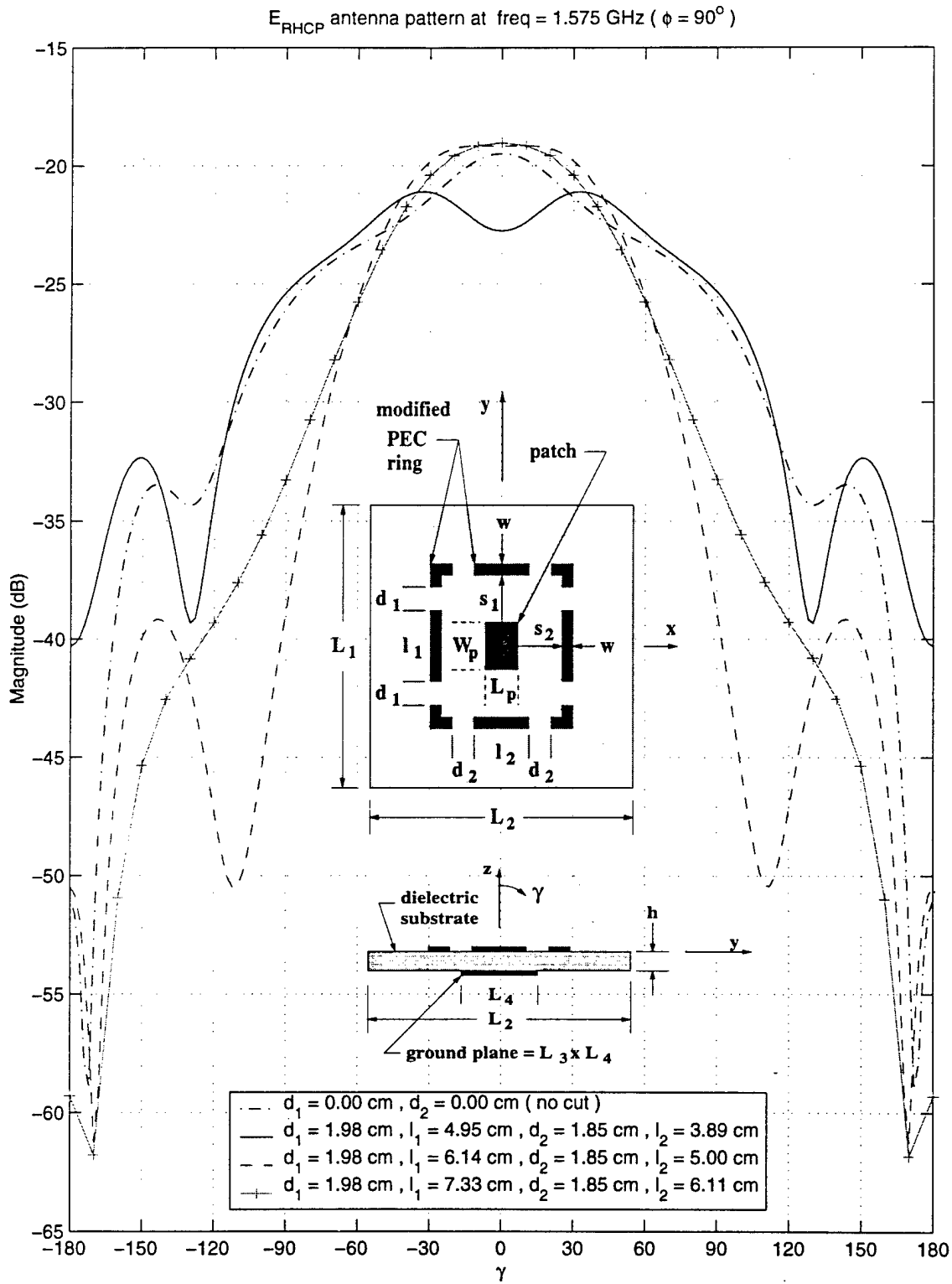


Figure 4.5: Radiation pattern of E_{RHCP} in $\pm 90^\circ$ plane as a function of ring dimensions l_1 and l_2 , L1 band

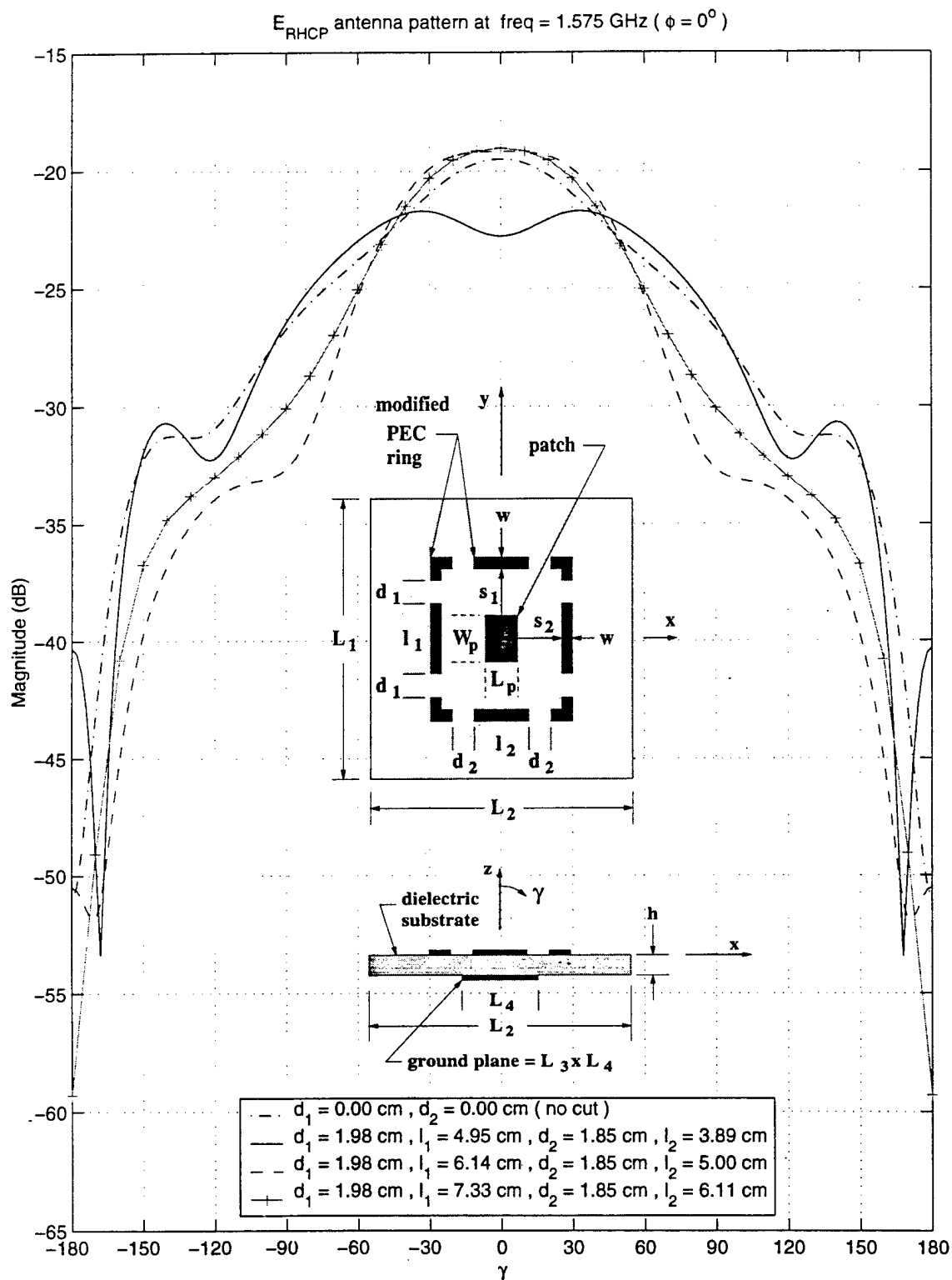


Figure 4.6: Radiation pattern of E_{RHCP} in $0^\circ - 180^\circ$ plane as a function of ring dimensions l_1 and l_2 , L1 band

4.3 Design of Metallic Ring for Simultaneous Operation at L1/L2 Frequencies

In this section, an example is presented to illustrate the application of the present scheme to two GPS antennas operating at L1 and L2, respectively. Figure 4.7 shows the ability of the present scheme to control the antenna pattern at 1.227 GHz, while Figure 4.8 shows the pattern control ability of the same ring structure applied to the 1.575 GHz RHCP microstrip antenna. The structure shown in the lower right corner of the two figures represents the state when all the switches are off. The structure shown in the lower left corner of the same two figures corresponds to the state when all switches are "on". When the switches are turned off, the beamwidths of the two right-hand circularly polarized antenna patterns (1.227 and 1.575 GHz) decrease and *vice versa*. In addition, the cross polarized (left-hand circularly polarized) patterns do not change significantly and remain at a low level as shown in Figures 4.9 and 4.10. Note that the cross polarized pattern levels may not be low enough, but this is mainly due to the design of the two circularly polarized antennas. Since the ability to adaptively control the antenna patterns is the main interest in the current research, the two RHCP microstrip antennas are not designed for optimum performance. A more sophisticated feeding structure may be required to improve the performance of the antenna elements, however, that is not the goal of this research effort. Figures 4.11-4.14 show the RHCP antenna patterns in the $0^\circ - 180^\circ$ plane and the corresponding cross-polarized antenna patterns for both GPS frequencies. It can be observed that the antenna patterns are not completely symmetric for the two orthogonal planes due to the asymmetry of the rectangular microstrip antenna used in these simulations. This deficiency can also be improved with a better feeding network. However, the goal of this study has clearly been met, namely, the ability to control in real time the antenna pattern beamwidth by using a parasitic metallic ring.

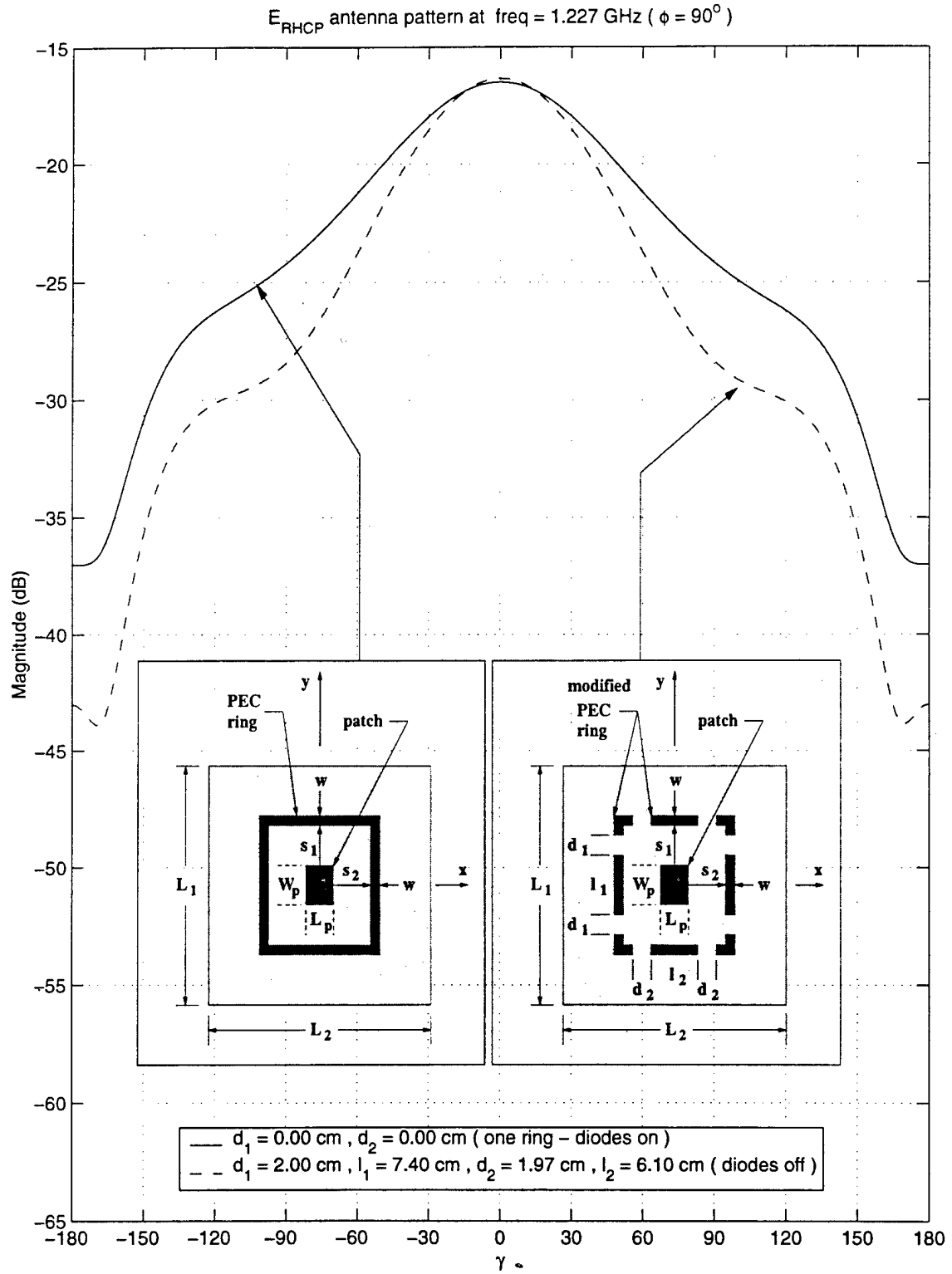


Figure 4.7: Calculated E_{RHCP} antenna pattern in $\phi = \pm 90^\circ$ plane at $f = 1.227$ GHz

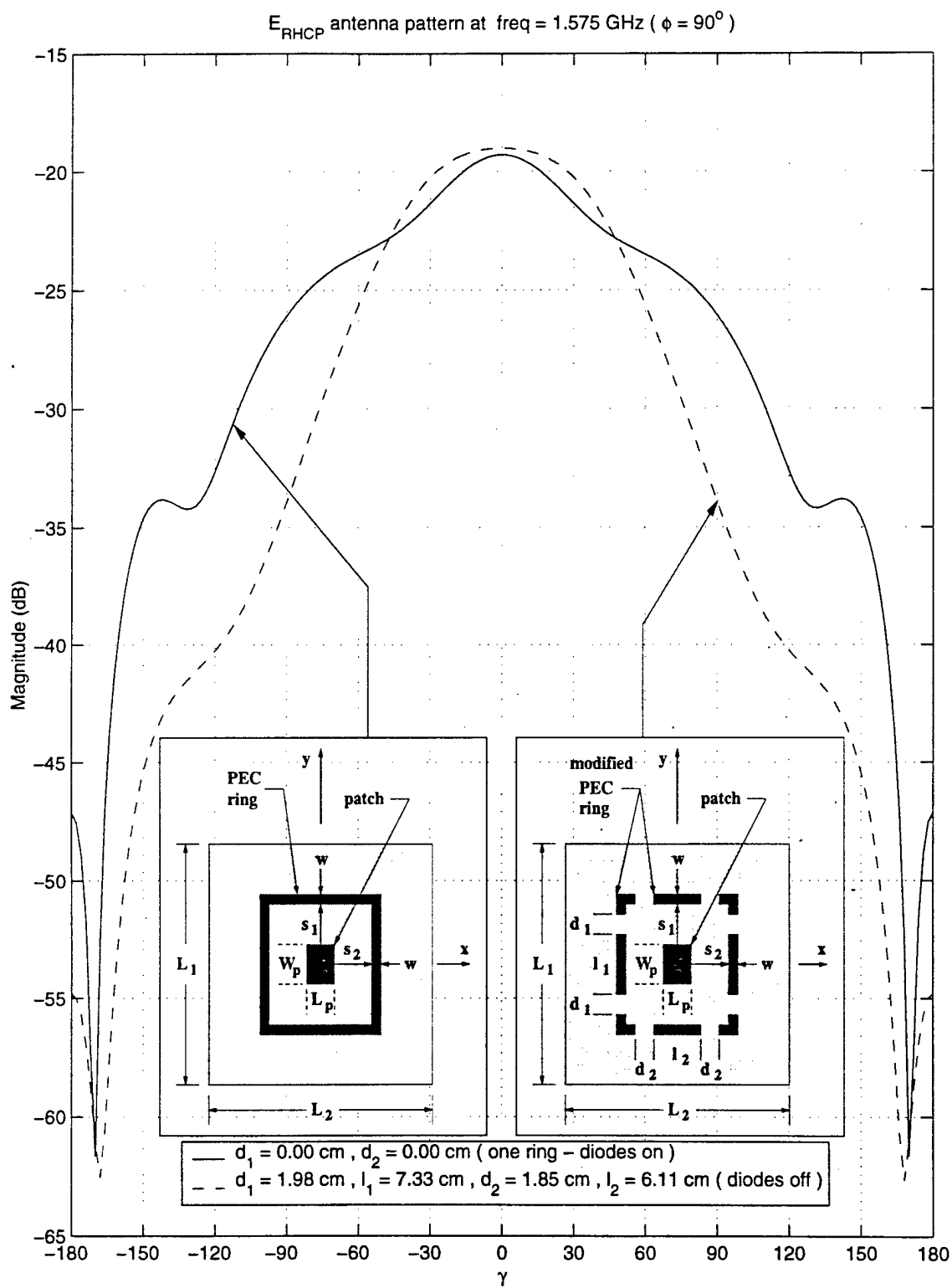


Figure 4.8: Calculated E_{RHCP} antenna pattern in $\phi = \pm 90^\circ$ plane at $f = 1.575$ GHz

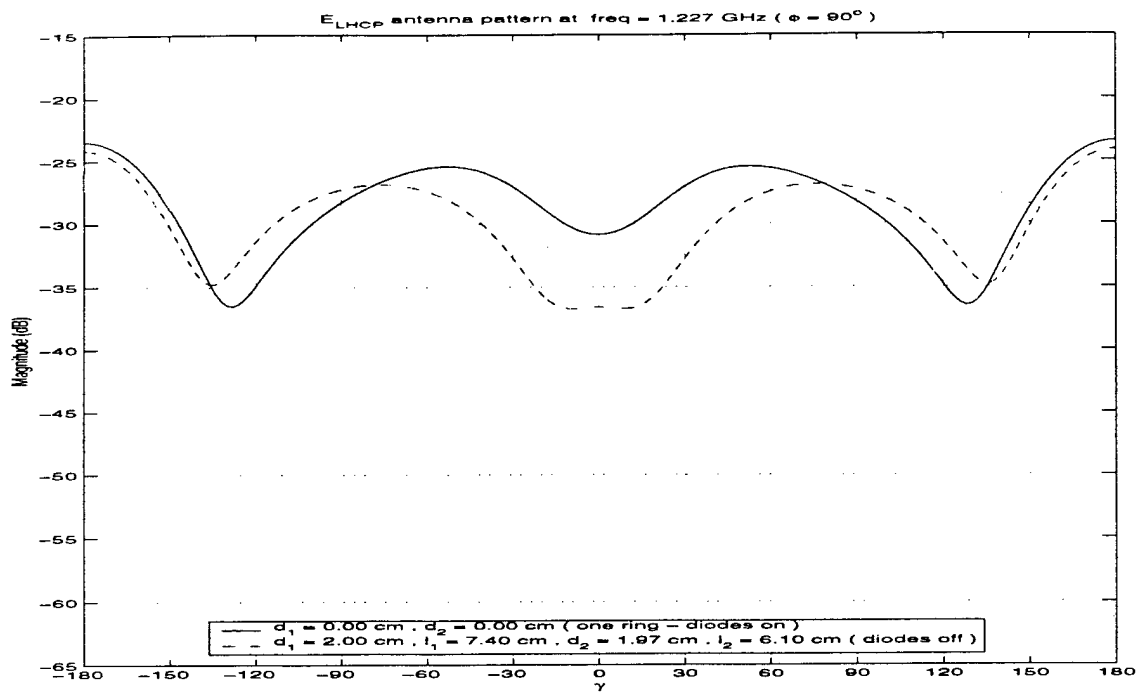


Figure 4.9: Calculated E_{LHCP} antenna pattern at $\phi = \pm 90^\circ$ at $f = 1.227$ GHz

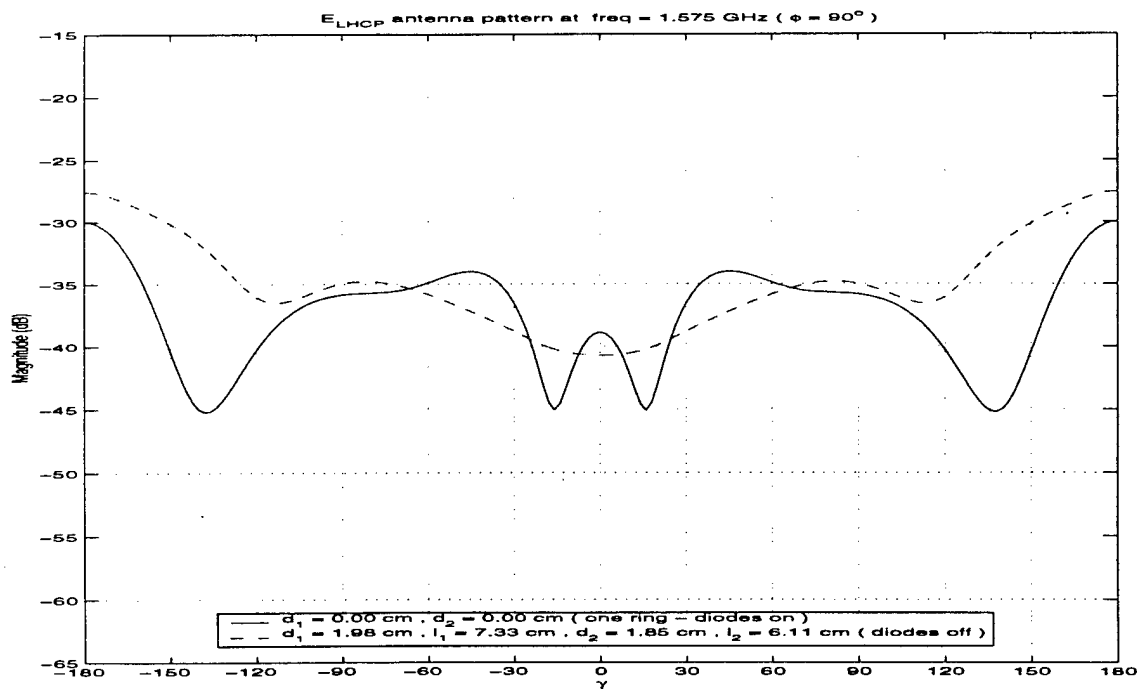


Figure 4.10: Calculated E_{LHCP} antenna pattern at $\phi = \pm 90^\circ$ at $f = 1.575$ GHz

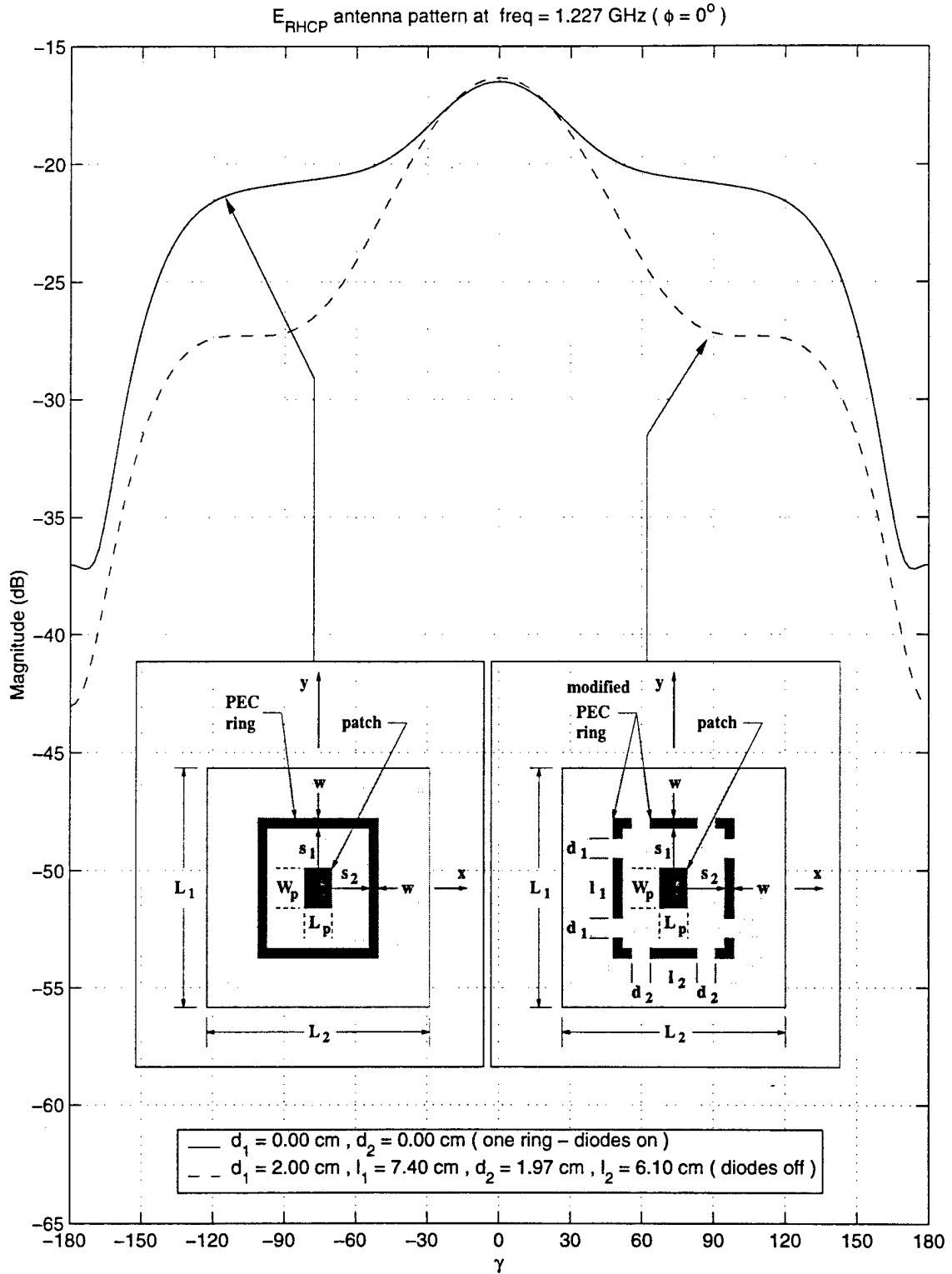


Figure 4.11: Calculated E_{RHCP} antenna pattern in $\phi = 0^\circ - 180^\circ$ plane at $f = 1.227$ GHz

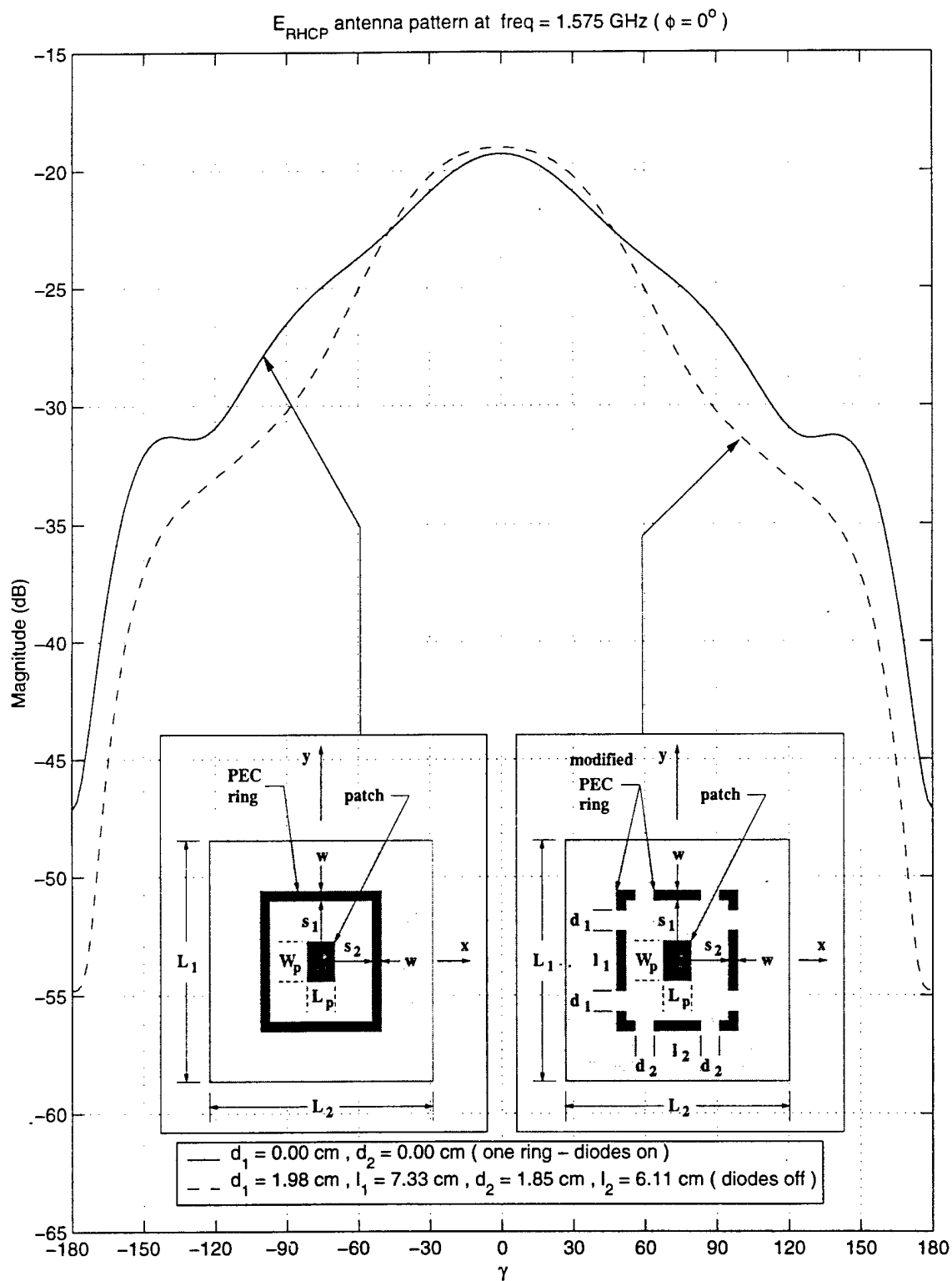


Figure 4.12: Calculated E_{RHCP} antenna pattern in $\phi = 0^\circ - 180^\circ$ plane at $f = 1.575$ GHz

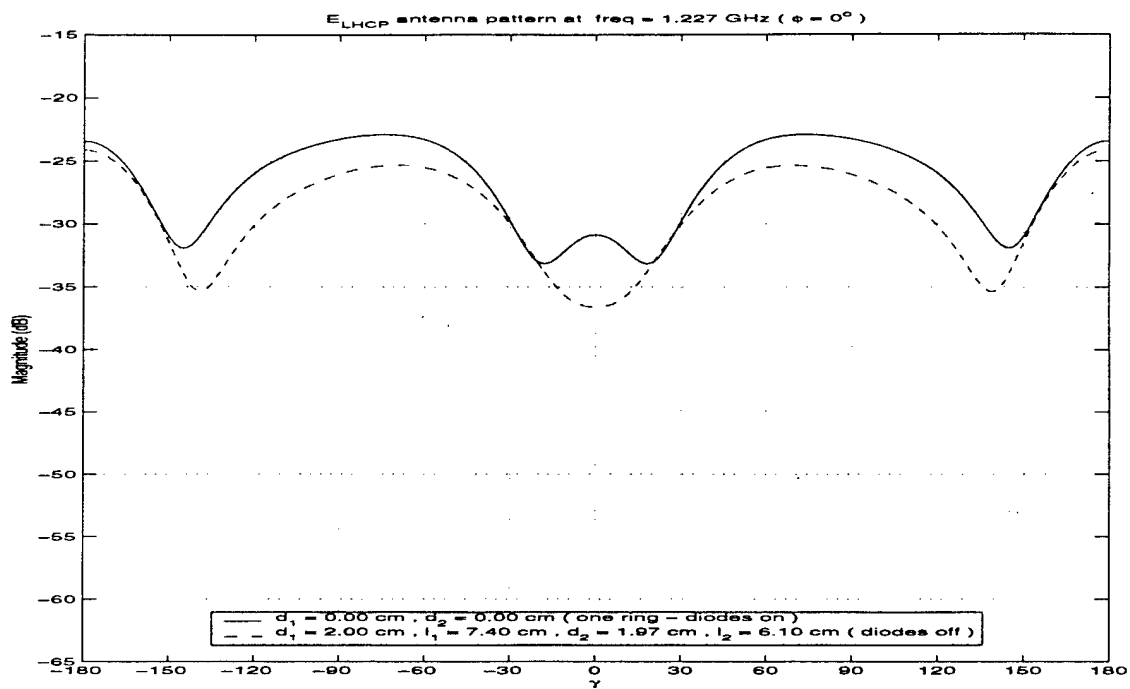


Figure 4.13: Calculated E_{LHCP} antenna pattern in $\phi = 0^\circ - 180^\circ$ plane at $f = 1.227$ GHz

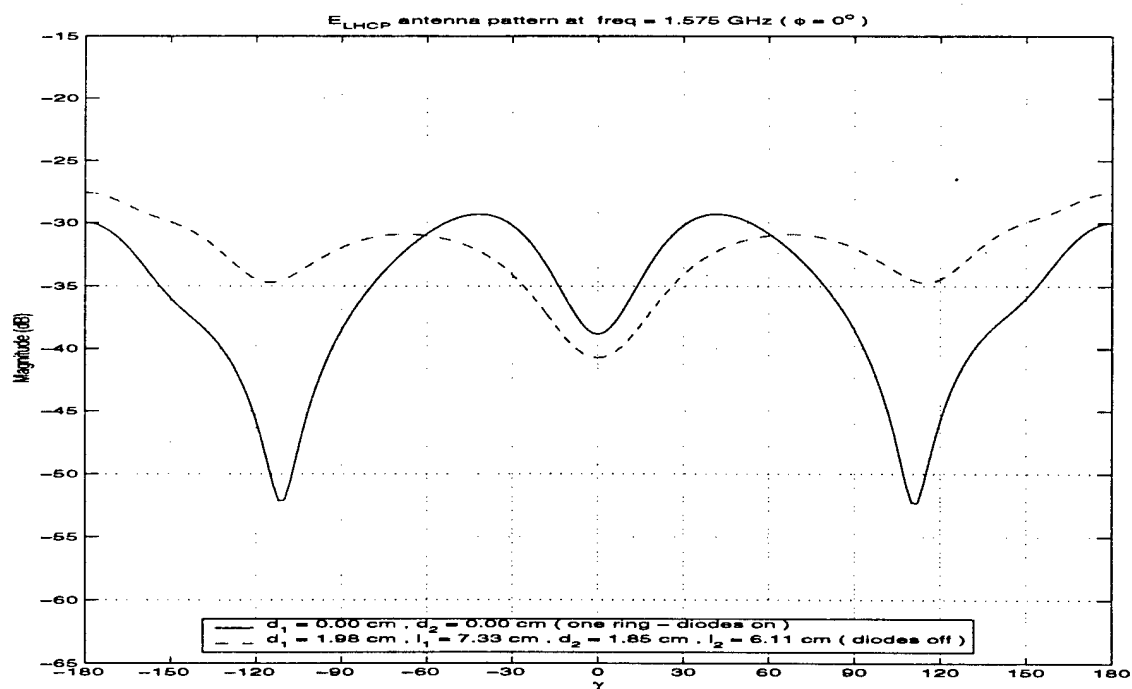


Figure 4.14: Calculated E_{LHCP} antenna pattern in $\phi = 0^\circ - 180^\circ$ plane at $f = 1.575$ GHz

Chapter 5

Summary and Conclusions

5.1 Accomplishments

In this report, several schemes to modify in real time the radiation patterns on linearly and circularly polarized printed antennas are presented. The basic idea is to add metallic strips around the radiating patch. The physical phenomenon behind these schemes is based on the control of surface waves excited on the substrate. These guided waves can be made to radiate in a controlled fashion by a proper design of the parasitic strips. Furthermore, the dimensions of the metallic strips can be changed in real time by using switches such as diodes, transistors or RF MEMS. This class of antennas are often referred to as reconfigurable antennas.

In Chapter 2, we presented the idea of using metallic strips connected with switches to control in real time the E- and H- plane patterns of linearly polarized microstrip antennas. In Chapter 3, a metallic-ring structure, also loaded with switches, was introduced. This structure is able to modify in real time the beamwidth of circularly polarized microstrip antennas at both GPS frequencies (1.227 and 1.575 GHz). One disadvantage of the above schemes is the overall size of the antenna. Thus, in Chapter 4, a smaller metallic-ring structure was introduced which is able to control the patterns of circularly polarized microstrip antennas. Based on preliminary results, this smaller structure seems to perform better than all the previous schemes. The main difference of the configurations presented in Chapters 3 and 4 is that in the latter, the ground plane of the patch is smaller than the parasitic ring. This results in

a portion of the substrate without any metallic cover or ground plane. This structure seems to be responsible for the overall reduction in size.

Although the overall size of the reconfigurable antenna structures introduced in this report is larger than the well known microstrip patch antenna by itself, it should be kept in mind that this reconfigurable antenna element can replace a traditional phased array antenna at a lower cost. Another important consideration that needs to be considered is the applicability of the above reconfigurable antenna elements for array applications. As mentioned in Chapter 1, if the antenna elements proposed here were to be used in an array, they would be designed with a high gain (narrow beamwidth) to avoid the problem of grating lobes. In other words, a reconfigurable antenna element would play the role of a sub-array in a large array configuration.

5.2 Suggestions for Future Work

The next step in this study will be the simulation of a GPS receiver, including the antenna of Chapter 4, in the presence of jamming signals. In contrast to most studies, the full wave model of the antenna will be included in the study.

Further study is still required to optimize the antenna introduced in Chapter 4. First of all, the selection of a dual frequency RHCP printed antenna, able to operate at the L1 and L2 frequencies is still pending. There are several designs found in the literature we are currently evaluating. Another alternative would be to design a wide band RHCP microstrip patch able to cover both GPS frequencies. There are a few wideband CP printed antennas found in the literature that we will also evaluate. The second aspect that still needs some further work is the optimum design of the parasitic ring, the placement and number of switches to be used.

Although it is not part of the present research effort, another aspect that needs to be considered in the future is the selection of the switches to actually implement a reconfigurable antenna element. As mentioned before, there are several alternatives (diodes, transistors, RF MEMS). The selection will be dictated by the cost and performance of the switches at the GPS frequencies. We are currently holding discussions

with experts in the field of switches to determine the best candidate for the present application.

Bibliography

- [1] N. Padros, J. I. Ortigosa, M. F. Iskander, and B. Thornberg, "Comparative study of high-performance gps receiving antenna designs," *IEEE Trans. Antennas Propagat.*, vol. 45, pp. 698-706, April 1997.
- [2] I. J. Bahl and P. Bhartia, *Microstrip Antennas*. Massachusetts: Artech House, 1980.
- [3] J. R. James, P. S. Hall, and C. Wood, *Microstrip Antenna Theory and Design*. IEE, London: Peter Peregrinus, 1981.
- [4] E. R. Brown, "Rf-mems switches for reconfigurable integrated circuits," *IEEE Trans. Microwave Theory Tech.*, vol. 46, pp. 1868-1880, Nov. 1998.
- [5] K. W. Lee and R. G. Rojas, "Study of novel adaptive printed antenna element using surface waves," *Dig. Int. Symp. Antennas Propagat. Soc.*, July 1999.
- [6] R. G. Rojas and K. W. Lee, "Study of Novel Adaptive Printed Antenna Element for GPS Applications," Tech. Rep. 735571-2, The Ohio State University ElectroScience Lab., March 1999.
- [7] R. Rojas and K. Lee, "Analysis and Design of Novel Adaptive Printed Antennas for GPS Applications," Tech. Rep. 737675-1, The Ohio State University ElectroScience Laboratory, December 1999.
- [8] V. B. Erturk, "Design and analysis of an active integrated transmitting antennas," M.S. Thesis, The Ohio State University, 1996.
- [9] W. F. Richards, *Microstrip Antennas*, ch. 10. NY: Van Nostrand Company, 1988.
- [10] K. R. Carver and E. L. Coffey, "Theoretical investigation of the microstrip antenna," Technical Report PT-00929, New Mexico State University Physical Science Laboratory, January 1979.
- [11] C. A. Balanis, *Advanced Engineering Electromagnetics*. NY: Wiley, 1989.